JPET Fast Forward. Published on May 3, 2010 as DOI: 10.1124/jpet.110.166363

Analgesic Effects of a Substituted N-Triazole Oxindole (TROX-1), a State-Dependant Ca_v2 Calcium Channel Blocker

Catherine Abbadie[‡], Owen B. McManus[‡], Shu-Yu Sun, Randal M Bugianesi, Ge Dai, Rodolfo J. Haedo, James B. Herrington, Gregory J, Kaczorowski, McHardy M. Smith, Andrew M. Swensen, Vivien A. Warren, Brande Williams, Stephen P. Arneric, Cyrus Eduljee, Terrance P. Snutch , Elizabeth W. Tringham, Nina Jochnowitz, Annie Liang, D. Euan MacIntyre, Erin McGowan, Shruti Mistry, Valerie V. White, Scott B. Hoyt, Clare London, Kathryn A. Lyons, Patricia B. Bunting, Sylvia Volksdorf, Joseph L. Duffy

Departments of Pharmacology (C.A., S-Y. S., N. J.; E. M.; E. M.; S. M., V. V. W.), Ion Channel Research (O. B. M., R. M. B., G. D., R. H., J. B. H., G. J. K., M. M. S., A. M. S., V. A. W., B. W.), Medicinal Chemistry (S. B. H., C. L., J. L. D.), and Drug Metabolism (K. A. L.), Merck Research Laboratories, Rahway, NJ, USA; Neuromed Pharmaceuticals, Vancouver, BC, Canada (S. P. A., C. E., T. P. S., E. W. T.); Departments of Pain Research (A. L.), and Safety and Exploratory Pharmacology P. B. B., S. V), Merck Research Laboratories, West Point, PA, USA

[‡]Contributed equally to this work.

JPET Fast Forward. Published on May 3, 2010 as DOI: 10.1124/jpet.110.166363
This article has not been copyedited and formatted. The final version may differ from this version.

Running Title: Analgesic effects of TROX-1, a state-dependent Ca_v2 blocker

Corresponding Author:

Dr. Joseph L. Duffy

Merck Research Laboratories

PO Box 2000

Rahway, NJ, 07065

Phone (732) 594-1062

FAX (732) 594-5966

Email joseph_duffy@merck.com

Number of text Pages 20

Number of Tables 4

Number of Figures 9

Number of References 40

Number of words in the Abstract: 237

Number of words in the Introduction: 492

Number of words in the Discussion: 1,336

Non-standard Abbreviations: BSA, bovine serum albumen; Ca_v, voltage-gated calcium channel; CBK, $Ca_v2.2$ HEK cell line; CFA, complete Freund's adjuvant; CGRP, calcitonin gene-related peptide; CNS, central nervous system; DMA, *N,N*-dimethylacetamide; DRG, dorsal root ganglia; GVIA, ω-conotoxin GVIA; HR, heart rate; IOA, iodoacetate; MVIIA, ω-conotoxin MVIIA; MAP, mean arterial pressure; MEM, minimum essential medium; NSAID, non-steroidal anti-inflammatory; PE, phenylephrine; PEG, polyethylene glycol; SNL, spinal nerve ligation; SNP, sodium nitroprusside; TROX-1, (3*R*)-5-(3-chloro-4-fluorophenyl)-3-methyl-3-(pyrimidin-5-ylmethyl)-1-(1*H*-1,2,4-triazol-3-yl)-1,3-dihydro-2*H*-indol-2-one.

Recommended section assignment: Neuropharmacology

JPET Fast Forward. Published on May 3, 2010 as DOI: 10.1124/jpet.110.166363
This article has not been copyedited and formatted. The final version may differ from this version.

Abstract

$Ca_v2.2$ (N-type) calcium channels are key components in nociceptive transmission pathways. Ziconotide, a state-independent peptide inhibitor of $Ca_v2.2$ channels, is efficacious in treating refractory pain but exhibits a narrow therapeutic window and must be administered intrathecally. We have discovered an N-triazole oxindole, TROX-1, as a small molecule state-dependent blocker of Ca_v2 channels, and investigated the therapeutic advantages of the compound for analgesia. TROX-1 preferentially inhibited potassium-triggered calcium influx through recombinant $Ca_v2.2$ channels under depolarized conditions (IC_{50}=0.27 μM) compared with hyperpolarized conditions (IC_{50}>20 μM). In rat dorsal root ganglion (DRG) neurons, TROX-1 inhibited ω-conotoxin GVIA-sensitive calcium currents ($Ca_v2.2$ channel currents) with greater potency under depolarized conditions (IC_{50}=0.4 μM) than under hyperpolarized conditions (IC_{50}=2.6 μM), indicating state-dependent $Ca_v2.2$ channel block of native as well as recombinant channels. TROX-1 fully blocked calcium influx mediated by a mixture of Ca_v2 channels in calcium imaging experiments in rat DRG neurons, indicating additional block of all Ca_v2 family channels. TROX-1 reversed inflammatory-induced hyperalgesia with maximal effects equivalent to non-steroidal anti-inflammatory drugs (NSAIDs), and reversed nerve-injury-induced allodynia to the same extent as pregabalin and duloxetine. In contrast, no significant reversal of hyperalgesia was observed in $Ca_v2.2$ gene-deleted mice. Mild impairment of motor function in the rota-rod test and cardiovascular functions were observed at 20-40-fold higher plasma concentrations than required for analgesic activities. TROX-1 demonstrates that an orally available state-dependent Ca_v2 channel blocker may achieve a therapeutic window suitable for the treatment of chronic pain.

JPET Fast Forward. Published on May 3, 2010 as DOI: 10.1124/jpet.110.166363
This article has not been copyedited and formatted. The final version may differ from this version.

Introduction

Inflammatory diseases and neuropathic insults are frequently accompanied by severe debilitating pain, which can become chronic and unresponsive to conventional analgesic treatments. Intrathecal administration of conventional agents, including morphine, may be required in more severe instances. Despite these aggressive treatment efforts, however, some patients remain refractory. A further intrathecal option is ziconotide, which is a synthetic peptide based on ω-conotoxin MVIIA (MVIIA) that selectively blocks neuronal-type (N-type) voltage-gated calcium channels. Intrathecal ziconotide has been approved for the management of chronic intractable pain, establishing block of N-type channels as the first new, proven mechanism for the treatment of chronic pain in many years (Miljanich, 2004).

N-type channels are encoded by the $Ca_v2.2$ calcium channel α_1 subunit and are largely restricted to the central and peripheral nervous systems (Dubel et al., 1992; Williams et al., 1992). Mapping studies reveal that N-type channels are located at key convergence points for nociceptive input to the central nervous system (CNS) on primary afferent terminals of sensory neurons in the superficial laminae of the dorsal horn (Westenbroek et al., 1998). The physiological roles of $Ca_v2.2$ channels have been investigated by utilizing a family of blocking polypeptides derived from the venom of marine cone snails, including ω-conotoxins MVIIA and GVIA (Olivera et al., 1994). Voltage-dependent opening of presynaptic $Ca_v2.2$ channels at primary afferent terminals allows the influx of extracellular Ca^{2+} ions, and this results in the release of glutamate, substance P, and calcitonin gene-related peptide (CGRP) from intracellular vesicles into the neuronal synapse. In this way, voltage-dependent Ca^{2+} entry directly modulates nociceptive input (Evans et al., 1996). In some pain states, expression of $Ca_v2.2$ channels is upregulated, suggesting an enhanced role for these channels in sensory signaling in chronic pain (Cizkova et al., 2002). Spinal administration of $Ca_v2.2$ blocking conopeptides profoundly attenuates hyperalgesia and allodynia resulting from nerve injury or inflammation in preclinical behavioral models of chronic pain (Malmberg and Yaksh, 1995; Scott et al., 2002). In addition, three separate strains of $Ca_v2.2$ gene knockout mice display reduced sensitivity to painful stimuli (Cao, 2006).

Ziconotide use is limited both by the method of delivery and a narrow therapeutic window

between analgesic efficacy and side effects (Miljanich, 2004). As a state-independent $Ca_v2.2$ blocker, ziconotide likely inhibits these channels under most conditions of electrical excitability, which may underlie the small therapeutic window (Winquist et al., 2005).

In the present study, we report the discovery of the *N*-triazole oxindole, TROX-1, a potent and state-dependent blocker of Ca_v2 channels ($Ca_v2.1$, $Ca_v2.2$, and $Ca_v2.3$) . TROX-1 efficacy was compared to drugs approved for inflammatory pain (NSAIDs) and neuropathic pain (pregabalin and duloxetine), and was shown to reduce nociception in preclinical pain models, while sparing normal cardiac and behavioral functions. However, TROX-1 afforded diminished efficacy in $Ca_v2.2^{-/-}$ mice, indicating that the analgesic activity of TROX-1 is primarily due to block of $Ca_v2.2$. These studies support the notion that an orally administered, state-dependent Ca_v2 blocker may have therapeutic utility in the treatment of chronic, severe pain.

Methods

Chemicals. TROX-1, (3*R*)-5-(3-chloro-4-fluorophenyl)-3-methyl-3-(pyrimidin-5-ylmethyl)-1-(1*H*-1,2,4-triazol-3-yl)-1,3-dihydro-2*H*-indol-2-one (Fig. 1) was synthesized at Merck Research Labs, Rahway, NJ. TROX-1 was diluted in Imwitor742:TWEEN80 (1:1) for oral administration, and in a mixture containing *N*-*N*-dimethylacetamide (DMA) and polyethylene glycol (PEG200) DMA:PEG200:water (40:40:20) for IV administration. Naproxen, indomethacin and diclofenac (Sigma, St. Louis, MI) were diluted in 0.5% methylcellulose (Sigma) in water. Pregabalin, and duloxetine (Sigma) were diluted in water. Ziconotide, sodium nitroprusside, and phenylephrine (Sigma) were diluted in saline for IV administration. Isradipine, ω-conotoxin GVIA, ω-agatoxin IVA, and SNX-482 were also obtained from Sigma.

Animals. In most studies, male Sprague-Dawley rats were utilized (220-350 g, Charles River Laboratories, Wilmington, MA). For the neuropathic pain models, Sprague-Dawley rats were purchased from Harlan (Indianapolis, IN). $Ca_v2.2$ deficient mice (described in Kim et al., 2001) were bred by Taconic (Hudson, NY). The procedures used in these studies were approved by the Institutional Animal Care and Use Committee at Merck and Co., Inc., Rahway, NJ, and adhere to the guidelines of the Committee for Research and Ethical Issues.

Fluorescence Assays. A fluorescent assay was used to measure compound-mediated inhibition of calcium influx with a calcium-sensitive florescent dye on a FLIPR Tetra^{TM} instrument. The assay is similar to that described (Dai et al., 2008) except that a different $Ca_v2.2$ cell line (labeled CBK) was used in the present work. CBK cells express three calcium channel subunits (α_{1B-1}, α_2-δ, $\beta_{3a,}$) along with an inward rectifier potassium channel ($Kir_{2.3}$) that enabled the cell membrane potential to be controlled by bath potassium concentration. Incubation of CBK cells in elevated potassium solution leads to depolarization of cell membrane potential. Exposing CBK cells to modestly elevated concentrations (30 mM) of potassium caused partial inactivation of the $Ca_v2.2$ channel population. In comparison, incubating cells in a bath solution containing 4 mM potassium maintained a negative membrane potential (-90 mV), at which voltage most $Ca_v2.2$ channels are in resting conformations. After compound incubation in 4 mM or 30 mM potassium, to evaluate block of resting and open / inactivated channels, respectively, channel opening was initiated with 1:1 (by volume) addition of 140

JPET Fast Forward. Published on May 3, 2010 as DOI: 10.1124/jpet.110.166363
This article has not been copyedited and formatted. The final version may differ from this version.

mM potassium solution. TROX-1 was tested in quadruplicate and average ±standard deviation values calculated for ten point titrations (0.001 to 30 μM).

Electrophysiological Experiments. Dorsal root ganglia (DRG) preparation: Dorsal root ganglia were dissected from 4-12 week old rats. Dissected ganglia from L4 to L6 were desheathed in ice-cold minimum essential medium (MEM) (Mediatech, Herndon, VA) and incubated in MEM containing 0.125% collagenase (type I) for 45-60 minutes at 37°C, followed by 0.05% trypsin for 10 minutes at 37°C. The ganglia were then washed in F14 growth media, consisting of 10% F14, 10% horse serum, 1% Pen/strep (5000 IU/500 μg) and 0.12% NaHCO3, and triturated with a fire-polished pipette to obtain a suspension with single cells. Cells were then maintained on a slow rotator for up to 6 hours until use.

DRG electrophysiology: Membrane currents were recorded using the whole-cell patch clamp technique with a HEKA (Port Washington, NY) EPC 10 patch-clamp amplifier. Fire-polished patch electrodes had resistances from 1-3 megaohms when filled with internal solution containing (in mM): 130 CsCl, 2.7 $MgCl_2$, 9 EGTA, 9 HEPES, 4 MgATP, 0.3 GTP(Tris), 14 phosphocreatine(Tris). External recording solution contained (in mM): 150 triethylammonium chloride, 5 $BaCl_2$, 0.5 $MgCl_2$, 10 HEPES, 10 glucose, pH 7.3 with triethylammonium hydroxide. Currents were leak subtracted using a standard p/4 subtraction protocol. To minimize the contribution of other non-$Ca_v2.2$ calcium channels present in DRG neurons, 100 nM isradipine, 300 nM agatoxin IVA, and 150 nM SNX-482 were added to the external solution. The standard voltage protocol consisted of a 100 msec prepulse to -50 mV to inactivate T-type channels followed by a 50 msec step to +10 mV, repeated once every 15 seconds, to activate $Ca_v2.2$ channels. Cells were first voltage clamped at a holding membrane potential of -90 mV. After a stable baseline was obtained, the holding potential was then stepped to either a more positive potential (-50 mV to -70 mV for ~30% channel inactivation) to measure $Ca_v2.2$ inhibition from a depolarized state, or to a more negative potential of -100 mV to estimate closed-state block. When a stable baseline was achieved at the new holding potential, compound was applied by bath perfusion until steady-state block was achieved. Peak currents were measured and the percent inhibition calculated using the current amplitude in 100 μM $CdCl_2$ (applied at the end of the experiment) as the baseline.

JPET Fast Forward. Published on May 3, 2010 as DOI: 10.1124/jpet.110.166363
This article has not been copyedited and formatted. The final version may differ from this version.

Calcium Imaging of Dorsal Root Ganglion Cells. Neonatal rat DRG neurons purchased from Lonza (Walkersville, MD) were grown on glass coverslips according to the manufacturer's instructions. The DRG neurons were loaded with fura-2 AM dye (2 μM, 30 min at room temperature) and perfused with a solution containing (in mM): 136 NaCl, 14 KCl, 1.8 $CaCl_2$, 0.5 $MgCl_2$, 10 glucose, 10 HEPES (pH 7.2). Isradipine (100 nM) was added to all solutions to remove any contribution of L-type, Ca_v1 channels. Images were collected with a Nikon TE200 inverted microscope equipped with a 40x S Fluor oil immersion objective (1.3 n.a.), an Orca-ER digital camera (Hamamatsu, Bridgewater, NJ) and a DG4 filter changer (Sutter Instruments, Novato, CA). Fura-2 was excited at 340 and 380 nm and fluorescence emission at 510 ± 20 nm captured. To trigger Ca_v channel opening, the bath solution was changed for 2 minutes to high potassium solution (in mM): 72 KCl, 78 NaCl, 1.8 $CaCl_2$, 0.5 $MgCl_2$, 10 glucose, 10 HEPES (pH 7.2 with NaOH), supplemented with 100 nM isradipine. The average fluorescence intensity ratio (R) in each cell body (F_{340}/F_{380}) was measured over time and the change in R (ΔR) for a potassium challenge was calculated by determining the peak R in high potassium and subtracting the baseline R just prior to potassium addition. Under these conditions, control experiments established that the DRG calcium signal was stable for up to 2 hours. On average, the calcium transient was 102 $\pm$ 3% (n=13) of the initial response after >100 min of control perfusion. Compound was added to cells for 20 min prior to potassium challenge and the fraction block calculated from the equation: $1-(\Delta R_{Drug}/\Delta R_{Control})$. The IC_{50} for block of ΔR was calculated from a fit to a standard Hill equation. Values are reported as mean ± SE.

To test the sensitivity of the DRG calcium signal to Ca_v2 block, the following protocol was used. After a single control stimulus, selective peptide inhibitors of $Ca_v2.2$ (ω-Conotoxin GVIA: 600 nM), $Ca_v2.1$ (ω-Agatoxin IVA: 300 nM), and $Ca_v2.3$ (SNX-482: 300 nM) were applied alone or in combination for >20 minutes prior to a second K stimulus and percent inhibition calculated.

ω-Conotoxin GVIA Binding Experiments. Membrane vesicles were prepared from rat lumbar spinal cords (Kuwayama and Kanazawa, 1982). Spinal cords (L4-L6) were removed and divided bilaterally in 2 hemi-sections ipsilateral and contralateral to a hind paw injected with complete Freund's adjuvant (CFA). In each experiment, sections from 4-8 animals were pooled and membrane vesicles from ipsilateral and contralateral sides were prepared in parallel. Conotoxin binding was performed

JPET Fast Forward. Published on May 3, 2010 as DOI: 10.1124/jpet.110.166363
This article has not been copyedited and formatted. The final version may differ from this version.

according to Feigenbaum (Feigenbaum et al., 1988). Samples were incubated overnight in 5 mL of sample buffer containing 50 mM TRIS-HCl, pH 7.4, 20 mM NaCl and 1 g/L bovine serum albumin (BSA), Fraction V, and increasing concentrations of ^{125}I-CgTX GVIA (2200 Ci/mmol; PerkinElmer Life and Analytical Sciences, Boston, MA). Non-specific binding levels were determined in the presence of 67 nM GVIA. Samples were diluted with 4 mL ice cold wash buffer containing 20 mM TRIS-HCl, pH 7.4, 30 mM NaCl and 0.06% BSA, and poured onto GFC filters preincubated for 15 min in 0.5% PEI for vacuum filtration. Filters were then washed twice with ice cold wash buffer. Radioactivity associated with the filters was determined in a Cobra gamma radiation counter. Binding values were normalized to protein concentrations using a commercially available protein assay (Pierce™BCA Protein Assay Kit, Pierce Biotechnology, Rockford, IL).

The ^{125}I-CgTX GVIA binding site densities for each membrane preparation were determined in saturation binding experiments repeated 2 or 3 times for each membrane preparation with close agreement between replicate measurements (average coefficient of variation=10.6%). The relative changes were averaged from six repeated experiments testing the effects of CFA treatment on ^{125}I-CgTX GVIA binding site density.

Ancillary Target Binding Assays. In-vitro binding assay screening for a panel of 166 ancillary targets was performed by MDS Pharma Services (King of Prussia, PA).

In vivo Pharmacology. TROX-1 was evaluated in well characterized in vivo models to assess acute, inflammatory, and neuropathic pain. Animals were randomly assigned to each treatment group. Results are presented as mean $\pm$ S.E.M. Percent Reversal are calculated as (post-dose – pre-dose)/(pre-injury-pre-dose)x100 for each rat. 100% corresponds to complete reversal of hyperalgesia or allodynia, equivalent to non-injured values, and 0% corresponds to values not different from baseline post-injury. Results were analyzed using a 2-way ANOVA (for dose and time post-dose) test followed by a Bonferroni post-tests for multiple comparisons (Prism, Graph Pad, San Diego, CA). ED_{50} are calculated as doses corresponding to a 50% effect (100% effect corresponding to recovery to baseline values in the absence of injury). Unless otherwise noted, all experimental and control groups contained at least six animals per group.

For the inflammatory pain model, rats were injected with CFA, 200 µL, 1:1 in saline; Sigma, St

Louis, MO) intraplantar into their left paw (Colpaert, 1987). Animals were tested for hyperalgesia 3 days after CFA administration, using withdrawal threshold to paw pressure (Randal-Sellito, Stoelting Co. Wood Dale, IL). To investigate whether the anti-hyperalgesic effect of TROX-1 was observed upon repeated dosing, the compound was administered for 3 days at 10 mg/kg QD in the CFA model of hyperalgesia. Reversal of mechanical hyperalgesia was assessed 3 hr post-dose on day 1, 2 and 3. Naproxen, indomethacin, and diclofenac (3-30 mg/kg PO) were included as a positive control.

For the neuropathic pain model (spinal nerve ligation, SNL), rats were anesthetized with isoflurane and were placed on a heating pad. Using aseptic techniques, the L5 spinal nerve was exposed, ligated and transected (Kim and Chung, 1992). Muscle and skin were closed with 4-0 Polydiaxone and wound clips, respectively. Allodynia was assessed 4 weeks post SNL surgery and only rats that developed allodynia as defined by a significant decrease in their mechanical threshold using von Frey filaments were used. Tactile allodynia was assessed with calibrated von Frey filaments (Stoelting Co, Wood Dale, IL), using an up-down paradigm (Chaplan et al., 1994). Pregabalin and duloxetine (3-30 mg/kg PO) were included as positive controls.

For the capsaicin-induced secondary allodynia model, rats were administered with capsaicin (intradermal, 30 µg in 10 µL, in ethanol:Tween80:saline 0.9%, (20:7:73)) 1 hr post-dose, and mechanical allodynia using von Frey filaments was assessed 30 min, 1 and 2 hr post-capsaicin. Percent inhibition of allodynia was calculated as: (post-drug – post-capsaicin) / (pre-capsaicin – post-capsaicin) x100, where 100% is equivalent to complete reversal of allodynia, i.e. pre-capsaicin value.

In the rat model of osteo-arthritis, iodoacetate (IOA, 2 mg/25 µL per rat in pH 7.4 saline; Sigma, St Louis, MO) was administered under brief isoflurane anesthesia into the rat left knee joint and hypersensitivity to von Frey filaments and changes in weight bearing were assessed 6 weeks post-IOA administration. Percent reversal of hypersensitivity was calculated as: (post-drug – post-IOA injection) / (pre-IOA injection – post-IOA injection)x100, where 100% is equivalent to complete reversal of hypersensitivity, i.e. pre-IOA injection value. Percent reversal of changes in weight bearing was calculated as: (post-drug – post-IOA injection) / (pre-IOA injection – post-IOA injection) x100, where 100% is equivalent to complete reversal of changes in weight bearing, i.e. pre-IOA injection value.

For the hot plate model of acute nociception, rats (male Sprague-Dawley Charles River, 170-

260 g; n=5 per group) were used. Latency time on a hot plate was assessed at 56 ^{o}C. Two baseline values 10 min apart were taken prior to compound administration. Rats were tested 1 and 3 hr after compound administration for changes in latency time.

For motor coordination assessment, rats were trained on the rota-rod (Stoelting Co.) for 3 minutes at a speed of 10 rpm. For testing, the speed was set at 10 rpm for 60 seconds and subsequently accelerated to 60 rpm. The time taken for rats to fall after the beginning of the acceleration was recorded.

For mouse CFA studies, mice (male from Taconic) received a unilateral 20 µL intraplantar injection of CFA (0.5 mg/mL, Sigma, St. Louis, MO) into the left paw. Thermal hyperalgesia (Hargreaves apparatus) was assessed 1 day post-CFA. Mice were habituated to the Hargreaves apparatus for 1 hr per day for 3 days before testing. Thermal sensitivity was assessed by measuring paw withdrawal latencies to a radiant heat stimulus. Mice deficient for $Ca_v2.2$ were initially characterized by Kim (Kim et al., 2001).

Measurement of Baroreflex Sensitivity. Rats were surgically implanted with cannulae (PE-50 tubing) in the left femoral artery and vein under aseptic conditions for the measurement of mean arterial pressure (MAP) and heart rate (HR) and administration of test agents, respectively. After 24h, the arterial catheter was connected to a DTX pressure transducer (Becton-Dickinson, Franklin Lake, NJ), which in turn fed into a universal signal conditioner (DSI, St. Paul, MN). The pressure signals were digitized and recorded on a computer utilizing the Ponemah data acquisition software (DSI, St. Paul, MN). The recorded data were reviewed offline and the MAP and HR were derived by the software for data analysis.

While animals were fully conscious and moving freely in their cages, sodium nitroprusside (SNP) or phenylephrine (PE) were administered as a bolus injection through the venous catheter to evoke changes in arterial pressure and baroreflex activity. A jugular catheter had to be placed for the administration of SNP and PE if the femoral vein catheter was occupied for administering test agent via a continuous infusion. A change of MAP from lowest to highest readings by at least 100 mm Hg was achieved by means of varying the doses of SNP from 8 to 32 µg/kg and of PE from 8 to 16 µg/kg. This was to ensure evaluation of the full range of baroreflex activities. SNP and PE were prepared

JPET Fast Forward. Published on May 3, 2010 as DOI: 10.1124/jpet.110.166363
This article has not been copyedited and formatted. The final version may differ from this version.

daily in saline at 100 µg/mL, and diluted to a final volume of 0.1 mL upon administration. The responses to SNP and PE in MAP and HR, averaged every second per data point, were plotted to fit a sigmoid function to establish the baroreflex function curve. The equation was described as HR = P1 + P2/[1 + $e^{P3(MAP-P4)}$], where P1 = low plateau of HR, P2 = HR range (difference between high and low plateaus), P3 = a curvature coefficient which is independent of HR range, and P4 = the median blood pressure (BP_{50}, mm Hg) at the point halfway between high and low HR plateaus. The average gain (G) or slope of the curve between the two inflection points is given by G = -P2 x P3/4.56 (Leppard et al., 1979).

To evaluate the effect of TROX-1 on baroreflex function, baseline baroreflex was characterized first at control condition as described above. Animals were then divided into three groups (n= 5 each) and treated with TROX-1 respectively at 0.1, 0.3 and 1 mg/kg/min via a 30-min IV infusion. Baroreflex evaluation was repeated at the end of the treatment and compared to that at control condition. Blood samples were taken after baroreflex function was measured to determine the plasma levels of the compound. An additional group of 4 rats were treated with vehicle (DMA:PEG200:water, 2:2:1) at matching volume and rate as control. To compare TROX-1 with a peptidyl $Ca_v2.2$ channel blocker, two groups of 4 rats were treated with GVIA at 1 and 3 µg/kg, respectively, administered as an IV bolus. Baroreflex function was measured prior to and 30 min after the toxin treatment. A third group of 3 rats was treated with saline as vehicle control.

Cardiovascular Study in Dogs. TROX-1 was administered intravenously to 3 anesthetized, vagotomized dogs during 3 sequential 30-minute periods at rising doses of 1, 2, and 7 mg/kg (cumulative dose 1, 3 and 10 mg/kg), in 50% dimethyl sulfoxide/50% polyethylene glycol 200 (v/v) to determine the effect of the compound on cardiovascular function. Dogs were anesthetized with sodium pentobarbital for the duration of the study. The right femoral artery and vein were cannulated for the measurement of mean arterial pressure and for maintenance of anesthesia respectively. The left femoral vein was cannulated for IV compound administration. Effects were compared to those of vehicle alone administered in a separate set of 4 dogs. Mean arterial pressure (MAP), heart rate (HR), and electrocardiographic parameters (PR, QRS, and QT/QTc intervals) were monitored pre-dose and during each 30-minute infusion. Blood was withdrawn at 29 min after the beginning of each infusion

interval, and collected in lithium heparin on ice, centrifuged, and plasma fraction removed and frozen (-70°C).

Plasma and Brain Level Analysis. Plasma and homogenized brain tissue concentrations of TROX-1 were determined by liquid chromatography / mass spectrometry (LC-MS/MS) using ABI Sciex API 3000 mass spectrometer operated in positive ion atmospheric pressure chemical ionization mode with multiple-reaction monitoring. Plasma and homogenized brain tissue were prepared for analysis by protein precipitation with acetonitrile. Extracts were chromatographed using a DuPont Zorbax SB-C8 column (50 x 2 mm, 5 micron) and eluted at 0.2 mL/min under isocratic conditions with acetonitrile:water (77:23) containing 5 mM ammonium formate/0.1% formic acid.

JPET Fast Forward. Published on May 3, 2010 as DOI: 10.1124/jpet.110.166363
This article has not been copyedited and formatted. The final version may differ from this version.

Results

TROX-1 Blocks $Ca_v2.2$ Channels in a State-Dependent Manner. TROX-1 (Fig. 1) was identified as a state-dependent $Ca_v2.2$ N-type channel blocker using the fluorescent calcium-influx assay. TROX-1 caused concentration-dependent inhibition of the calcium influx signal and inhibited channel activity more effectively in recombinant cells under conditions in which the cells were depolarized (30 mM bath potassium; IC_{50}=0.27 ± 0.13 μM, n=8) than when cells were hyperpolarized (4 mM bath potassium; IC_{50}>10 μM, n=4). In the representative experiment shown in Figure 1, the IC_{50} for $Ca_v2.2$ inhibition under depolarized conditions (0.25 μM; Fig.1A) was approximately 100-fold lower than for channel inhibition under hyperpolarized conditions (~28 μM; Fig. 1B). The amplitude of the peak calcium influx signal is smaller in Fig. 1A (30 mM K) than in Fig. 1B (4 mM K) due to inactivation of a fraction of the $Ca_v2.2$ channels.

TROX-1 Inhibits $Ca_v2.2$ Channels in Isolated DRG Neurons. Calcium channel currents in rat DRG neurons were recorded in electrophysiology experiments with barium as the charge carrier. Contributions from non-$Ca_v2.2$ calcium channels were minimized by using a mixture of pharmacological blockers and voltage pre-pulses. The average current inhibited by 600 nM GVIA after minimizing non-$Ca_v2.2$ currents was 85 ± 1% (n=4) from depolarized holding potentials and 82 ± 1% (n=4) from hyperpolarized holding potentials. When cells were depolarized to obtain a ~30% inactivation of Ca_v current (V_{hold} = -50 mV to -70 mV), 300 nM TROX-1 inhibited 47 ± 2% (n=5) and 1 μM TROX-1 inhibited 69 ± 4% (n=3) of the DRG barium current. Consistent with a state-dependent blocker, when cells were held hyperpolarized (V_{hold} = -100 mV) to minimize open/inactivated-state block, 1 μM TROX-1 inhibited only 28 ± 3% (n=5) and 3 μM TROX-1 inhibited 54 ± 6% (n=4) of the DRG barium current. A Hill fit of data from an expanded titration of TROX-1 yielded an estimated IC_{50} of 0.4 μM for the depolarized inhibition and 2.6 μM for the hyperpolarized inhibition (Fig.1C).

As a measure of the functional effects of TROX-1 on other Ca_v2 channels in rat DRG neurons, fura-2 calcium imaging of neonatal DRGs was performed. To detect state-dependent Ca_v channel block, DRGs were bathed in an elevated potassium solution (14 mM) to modestly depolarize the membrane (Vm ≅ -58 mV). Isradipine (100 nM) was added to all solutions to remove any contribution of Ca_v1 (L-type) channels. Under these conditions, studies with individual toxins and paired

combinations suggest that $Ca_v2.2$ channels contribute significantly to the overall signal (Table 1). However, the peak Ca transient triggered by application of 72 mM potassium solution was inhibited to the greatest extent by a combination of GVIA, ω-Agatoxin IVA and SNX-482, which selectively block $Ca_v2.2$, $Ca_v2.1$ (P/Q-type) and $Ca_v2.3$ (R-type) channels, respectively (81% block in the representative experiment in Fig. 2A) (Doering and Zamponi, 2003). These results suggest that the calcium rise was driven by the opening of multiple Ca_v2 channel subtypes. TROX-1 dose-dependently reduced the Ca transient (Fig. 2B) with an estimated IC_{50} of 2.1 μM (Fig. 2C) and blocked nearly all the signal at maximal TROX-1 concentrations.

TROX-1 Selectively Inhibits Ca_v2 Channels Over Ancillary Targets. Block of $Ca_v1.2$ (L-type) channels and $Ca_v3.1$ and $Ca_v3.2$ (T-type) channels was determined in similar fluorescent calcium-influx assays (Table 2). TROX-1 displayed weak block of these calcium channel subtypes compared with block of $Ca_v2.2$. TROX-1 afforded selectivity for $Ca_v2.2$ over sodium channel targets relevant to analgesia, including $Na_v1.7$ and $Na_v1.8$, in voltage-based fluorescent assays. TROX-1 was also selective over cardiac ion channels in electrophysiological experiments, with weak block of $Na_v1.5$, I_{kr}, and I_{ks}.

In an additional screen of 166 targets, 10 μM TROX-1 exhibited activity (>50% inhibition) in only three binding assays. TROX-1 was active in the adrenergic α_{2A} binding assay, with an IC_{50} of 8.2 μM. In a subsequent GTPγS functional assay for α_{2A} activity, TROX-1 exhibited no agonist activity and weak antagonist activity, with maximal 35% functional inhibition at 10 μM. TROX-1 was also active in the serotonin 5-HT_6 binding assay, with an IC_{50} of 8.8 μM. In a subsequent cAMP functional assay for 5-HT_6 activity, the compound exhibited no agonist activity and weak antagonist activity, with maximal 49% functional inhibition at 10 μM. Finally, TROX-1 was active as an inhibitor of PDE4, with an IC_{50} of 7.6 μM.

Pharmacokinetic Properties. In rats, TROX-1 afforded good bioavailability (F=89%) after oral (PO) administration of 3 mg/kg with a maximal concentration (C_{max}) of 2.1 μM obtained 0.8 h post-dose (T_{max}). Following an intravenous (IV) dose of 1 mg/kg, TROX-1 exhibited a moderate plasma clearance rate of 13 mL/min/kg and with a half-life of 2.2 h. With PO administration, TROX-1 plasma exposure increased in a dose proportional manner between 1 and 100 mg/kg. Further, TROX-1 was

found to be brain penetrant, with similar compound concentrations found in homogenized brain and plasma at all doses and times examined.

Spinal $Ca_v2.2$ Density Increase Ipsilateral to Injury. Inflammatory pain was induced by intra-plantar injection of complete Freund's adjuvant (CFA) into a single hind paw of rats. Three days after CFA injection, a significant 32 $\pm$ 14% (mean $\pm$ SD, n=6 experiments) increase in ^{125}I-CgTX GVIA binding was observed in the rat spinal cord (L4-L6 membrane vesicles) ipsilateral to CFA treatment as compared with the contralateral side (Fig. 3). The site densities increased from 0.225 $\pm$ 0.013 pmoles/mg protein on the contralateral sides to 0.297 $\pm$ 0.032 pmoles/mg protein on the ipsilateral sides. These differences were significant at the $p<0.01$ level assessed by the paired t-test.

TROX-1 Exhibits Antinociceptive Activity. TROX-1 was evaluated after PO administration in standard rodent models of chronic pain and its anti-nociceptive activity was compared to analgesics currently used therapeutically. In the rat CFA model, a single dose of either TROX-1, vehicle, or a non-steroidal anti-inflammatory drug (NSAID) was administered, and mechanical hyperalgesia was assessed at 1, 3, 8 and 24 hr post-dose. TROX-1 dose-dependently reversed CFA-induced hyperalgesia (Fig. 4A) with a maximal effect of 81% reversal (100% corresponding to non-inflamed condition) at 30 mg/kg, and a duration of action greater than 8 hr post-dose at 3 mg/kg. The magnitude of efficacy of TROX-1 at the 1h time point was equivalent to analgesics used for inflammatory pain, such as naproxen, diclofenac or indomethacin (Fig. 4B).

Sustained reversal of rat CFA-induced hyperalgesia was observed following chronic administration of TROX-1 (Fig. 5). TROX-1 at 3 hr post-dose induced similar reversal of hyperalgesia on all days (52% on day 1, 57% on day 2, and 58% on day 3). Controls included rats that received vehicle for 2 days and TROX-1 on day 3. The reversal of hyperalgesia was similar after 3 day dosing of TROX-1 (58%) to dosing of TROX-1 only on day 3 (54%). Plasma levels of TROX-1 were measured at 3 hr following each dose in this experiment, and found to be 2.76 µM on day 1, 3.65 µM on day 2, and 3.41 µM on day 3.

In the rat capsaicin-induced secondary allodynia model of central sensitization, TROX-1 dose-dependently reversed allodynia to the same magnitude as pregabalin and duloxetine, drugs approved for the treatment of diabetic neuropathy (Fig. 4C). In the rat Spinal Nerve Ligation (SNL) model of

JPET Fast Forward. Published on May 3, 2010 as DOI: 10.1124/jpet.110.166363
This article has not been copyedited and formatted. The final version may differ from this version.

neuropathic pain, in which compounds are evaluated four weeks after ligation, TROX-1 dose-dependently reversed mechanical allodynia (Fig. 4D). Maximal reversal of allodynia (72%) was observed at the 30 mg/kg dose. The magnitude of this effect was similar to that of both pregabalin and duloxetine (Fig. 4E). Estimated ED_{50} values for TROX-1, pregabalin and duloxetine in the SNL neuropathic pain model were 8, 7 and 4.5 mg/kg, respectively (Fig. 4E).

TROX-1 efficacy was also assessed in rats in the knee intra-articular iodo-acetate (IOA) model of osteoarthritis. TROX-1 reversed IOA-induced allodynia (Fig. 6A): 17, 27 and 49% at 3, 10 and 30 mg/kg, respectively at 1 hr post-dose. By comparison, naproxen at 20 mg/kg reversed allodynia by 47% in this assay. TROX-1 also reversed IOA-induced weight-bearing (Fig.6B): 28, 38 and 43% at 3, 10 and 30 mg/kg, respectively at 1 hr post-dose. Naproxen administered at 20 mg/kg reversed weight-bearing effects by 42% in this assay.

In a model of acute nociception (rat hot-plate at 56 °C), TROX-1 administered orally at 10 or 30 mg/kg had no effect on thermal threshold at 1 or 3 hr post-dose. Morphine administered subcutaneously at 10 mg/kg significantly increased thermal thresholds 1 hr post-dose (Fig. 7).

In order to assess the contribution of $Ca_v2.2$ blockade on the antinociceptive activity of TROX-1 over blockade of related Ca_v2 channels, we evaluated the compound for the reversal of CFA-induced hypersensitivity to heat in mice lacking only $Ca_v2.2$ channels. As previously reported (Kim et al., 2001) we found that $Ca_v2.2$ deficient mice showed a significantly greater thermal threshold as compared to wild-type mice in the absence of injury (pre-CFA, Fig. 4F). Hyper-sensitivity to heat was measured in both $Ca_v2.2^{+/+}$ and $Ca_v2.2^{-/-}$ mice given intra-plantar injections of CFA to induce inflammatory pain. $Ca_v2.2$ deficient mice showed a significant reduction (50% vs. 71% decrease in latency) in hyperalgesia as compared to control mice (CFA, Fig. 4F). TROX-1 significantly reversed CFA-induced hyperalgesia in wild type mice (88% reversal), but did not significantly reduce hyperalgesia in $Ca_v2.2$ deficient mice (31% reversal; Fig. 4F).

TROX-1 In Vivo Side Effect Profile. In the rat rota-rod model of motor coordination, pregabalin and duloxetine induced significant impairment (>20%) of balance at doses greater than 30 mg/kg. At higher dosing (100 mg/kg) pregabalin and duloxetine reduced rota-rod performance by 61% and 45%, respectively (Fig. 4E). In contrast, TROX-1 did not induce detectable motor impairment at 30 mg/kg

PO although a significant, but mild impairment was apparent at 100 mg/kg (21% inhibition as compared to baseline). In order to determine the CNS therapeutic window of TROX-1 and compare it to standard analgesics, we calculated the ratio of rota-rod ED_{20} / SNL ED_{50}. In the rota-rod model, pregabalin and duloxetine ED_{20} values, corresponding to significant motor-coordination impairments, were 15 and 45 mg/kg, respectively (Fig. 4E). Using these criteria and data, the CNS therapeutic window was estimated to be ~2 for pregabalin and ~10 for duloxetine (Fig. 4E). Significant motor effects with TROX-1 were only observed at 100 mg/kg, providing an estimated CNS therapeutic window of ~12.5. The therapeutic window for TROX-1 was also estimated based on plasma exposure achieved in these assays. The EC_{50} values for TROX-1 in rat pain models were ~1 μM and rota-rod effects were observed at ~20 μM, providing a CNS therapeutic window of 20 fold (Fig. 8A).

Cardiovascular Activity of TROX-1. Both TROX-1 and GVIA were evaluated in baroreflex models in conscious rats to determine the potential of these agents to induce orthostatic hypotension. GVIA was initially evaluated for potential hemodynamic effects in conscious rats to help identify dose selection for baroreflex studies. GVIA (1-30 μg/kg i.v.) evoked a modest decrease in heart rate (HR) (~10%) and a profound decrease in mean arterial pressure (MAP) (>30%) at doses of 10 and 30 μg/kg. Accordingly, the maximum dose of GVIA evaluated for effects on baroreflex sensitivity was 3 μg/kg.

Baroreflexes were elicited in conscious rats via acute administration of phenylephrine (PE) to increase MAP, or sodium nitroprusside (SNP) to decrease MAP, while evaluating the corresponding changes in heart rate. In control animals, baseline MAP was 116 $\pm$ 6 mm Hg and HR was 450 $\pm$ 11 beats/min. The administration of PE increased MAP to 175 $\pm$ 6 mm Hg with a corresponding decrease in heart rate to 320 $\pm$ 11 beats/min, and the administration of SNP decreased MAP to 61 $\pm$ 6 mm Hg with a corresponding increase in heart rate to 531 $\pm$ 17 beats/min. From plots of heart rate against MAP, the heart rate range (difference between high and low plateaus) and the rate of change (gain) in heart rate were calculated with respect to changes in MAP, using the sigmoid function described in the Methods. The median blood pressure (BP_{50}, mm Hg) was also calculated at the point halfway between the high and low heart rate plateaus, and the values from this curve fit are presented in Table 3. GVIA (3 μg/kg) evoked significant decreases in heart rate range and in the gain function as compared to vehicle control (Fig. 9A). In contrast, none of the baroreflex parameters were significantly

altered by the infusion of TROX-1 at 0.1 or 0.3 mg/kg/min, corresponding to plasma levels of 2.5 $\pm$ 0.5 μM and 14 $\pm$ 2.5 μM, respectively (Table 3). The heart rate range was reduced by TROX-1 at 1 mg/kg/min (plasma level = 38 $\pm$ 4 μM) however, the average gain was not changed at this highest dose (Fig. 9B).

In order to further characterize the cardiovascular properties, TROX-1 was administered intravenously in sequential rising doses to anesthetized, vagotomized dogs (Table 4). At 1 mg/kg (administered over 30 min) there were no significant effects on MAP or heart rate as compared to effects with vehicle alone. At 3 mg/kg and 10 mg/kg (cumulative doses) TROX-1 dose-dependently decreased MAP (-10% and -25%) and heart rate (-16% and -20%). TROX-1 also slightly increased the PR interval (< 9%) over the dose range, which may be secondary to the decrease in heart rate. There were no treatment-related effects on QRS or QTc cardiac intervals up to a maximum mean exposure of 55 ± 21 μM following the 10 mg/kg cumulative dose.

The cardiovascular therapeutic window of TROX-1 was determined using the ratio of dog or rat cardiovascular side effect EC_{20} / rat analgesic effect EC_{50}. In the anesthetized dog cardiovascular studies, 20% change from baseline in heart rate and MAP corresponded to 55 and 40 μM, respectively (Fig. 8B). In rat baroreflex studies, heart rate range was only significantly reduced at the highest dose of 1 mg/kg/min, corresponding to plasma levels of ~38 μM. Therefore, TROX-1 exhibited a cardiovascular therapeutic window of ~38-fold.

JPET Fast Forward. Published on May 3, 2010 as DOI: 10.1124/jpet.110.166363
This article has not been copyedited and formatted. The final version may differ from this version.

Discussion

The present findings using the *N*-triazole oxindole, TROX-1, show that an orally bioavailable, state-dependent Ca_v2 blocker is efficacious in preclinical pain models, while preserving normal neurologic and hemodynamic functions. The analgesic effects of oral doses of TROX-1 were established in several preclinical models of chronic pain in rats, including the CFA model of inflammatory pain and the intra-articular iodoacetate model of osteoarthritis, with efficacy similar to the anti-inflammatory agents naproxen, indomethacin, and diclofenac. TROX-1 was similarly active in the SNL (Chung) model of neuropathic pain, with efficacy similar to the analgesic agents pregabalin, which binds to the $\alpha2\delta$ subunit of calcium channels, and duloxetine, which is a dual serotonin and norepinephrine reuptake inhibitor. The precise mechanisms by which the latter two therapies affect spinal neurotransmission are under active research (Tsukamoto et al., 2010, and references cited therein). TROX-1 analgesic activity was abrogated in mice deficient for $Ca_v2.2$, suggesting that its efficacy is derived primarily by block of $Ca_v2.2$ channels.

At analgesic doses, TROX-1 produced no observable changes in motor coordination, cardiovascular function, or hemodynamic parameters. TROX-1 did induce mild impairments at 20-40-fold higher doses or plasma concentrations. These findings indicate that a state-dependent Ca_v2 blocker affords a substantially greater therapeutic window for neurologic and hemodynamic effects as compared to ziconotide.

State-Dependent $Ca_v2.2$ Channel Block Provides Functional Selectivity. Data from the present study demonstrate an increase in $Ca_v2.2$ channel density in the rodent lumbar spinal cord subsequent to an inflammatory pain state (Fig. 3), suggesting an enhanced role for $Ca_v2.2$ channels in inflammatory pain signaling. Similar results have been reported by studying a rodent neuropathic pain model using immunocytochemistry to measure $Ca_v2.2$ channel density after nerve injury (Cizkova et al., 2002). Both genetic and pharmacological data provide additional evidence that reducing $Ca_v2.2$ channel activity attenuates nociceptive signaling, but this also impacts cardiovascular function. $Ca_v2.2$ knockout mice display reduced hyperalgesia in the CFA model (Fig. 4F), and reduced response to noxious mechanical, thermal, chemical and inflammatory visceral stimuli (Kim et al., 2001). Peptides, including GVIA, which block $Ca_v2.2$ channels in a state-independent manner (Dai et al., 2008), are

active in reducing tactile allodynia and thermal hyperalgesia in a nerve injury model (Wang et al., 2000; Scott et al., 2002) and attenuate nociceptive responses in inflammatory pain models (Malmberg and Yaksh, 1995; Bowersox et al., 1996). These peptides inhibit excitatory synaptic transmission between primary afferent sensory neurons and superficial laminae dorsal horn neurons (Heinke et al., 2004; Motin and Adams, 2008) and inhibit excitation of dorsal horn neurons by noxious sensory stimulation (Diaz and Dickenson, 1997). Data derived from $Ca_v2.2$ knockout mice and $Ca_v2.2$-blocking peptides have also provided evidence for important roles for $Ca_v2.2$ channels in cardiovascular functions. $Ca_v2.2^{-/-}$ mice display reduced atrial positive ionotropic responses to sympathetic stimulation, reduced baroreflex responses, and surprisingly, elevated mean arterial pressures and heart rates (Ino et al., 2001; Mori et al., 2002). Systemic administration of ziconotide, and related peptides that block $Ca_v2.2$ channels, also impair cardiovascular functions including decreased mean arterial pressure, orthostatic hypotension and attenuated baroreflex responses (Bowersox et al., 1992; Pruneau and Belichard, 1992; Wright and Angus, 1995; Wright et al., 2000).

State-dependent block of $Ca_v2.2$ channels by TROX-1 afforded a different *in vivo* profile than observed after state-independent channel block by peptides. TROX-1 provided clear antinociceptive activity in models of inflammatory and neuropathic pain, at plasma concentrations (EC_{50}=1 μM) and doses (ED_{50}=10 mg/kg PO) that did not cause significant changes in central nervous system (rota-rod) or cardiovascular functions. Concentrations of TROX-1 were similar in brain and plasma, indicating that the differential effects on nociceptive and other functions do not result from concentration differences in different tissues. Significant motor effects of TROX-1 were only observed at plasma concentrations above 20 μM and cardiovascular effects were seen above 38 μM. The state-dependent nature of $Ca_v2.2$ block by TROX-1 may underlie the selective modulation of nociceptive responses compared with cardiovascular and motor functions. The activity of $Ca_v2.2$ channels will be governed by the local profile of electrical activity and by other regulatory processes, and may differ across sites and physiological conditions. Depolarization or higher action potential frequencies may occur in sensory axon terminals following injury (Vyklicky et al., 1969). $Ca_v2.2$ blockers that preferentially block open or inactivated channels could inhibit this enhanced nociceptive signaling while preserving other neuronal functions. However, the precise relationship between the degree of

JPET Fast Forward. Published on May 3, 2010 as DOI: 10.1124/jpet.110.166363
This article has not been copyedited and formatted. The final version may differ from this version.

state-dependence for $Ca_v2.2$ block and the magnitude of the therapeutic window remains to be established.

Implications of Non-Selective, State-Dependent Block of All Cav2 Channel Subtypes by TROX-1. TROX-1 blocked calcium influx in DRG neurons that was mediated by a combination of all Cav2 channel subtypes, and experiments with recombinant $Ca_v2.1$, $Ca_v2.2$ and $Ca_v2.3$ channels revealed similar block of these channel subtypes by TROX-1 (manuscript in preparation). The roles of Cav2 channel subtypes have been examined using genetic and pharmacological approaches that often serve to completely abrogate channel function, or rely on human mutations for which the link between the mutations and the phenotypes are not fully understood. $Ca_v2.1^{-/-}$ mice die 3-4 weeks following birth and display ataxia, dystonia, absence seizures, cerebellar degeneration, decreased responses in inflammatory pain models and altered sensory processing prior to death (Jun et al., 1999). A variety of human $Ca_v2.1$ mutations produce profound CNS effects, including episodic ataxia and absence epilepsy (loss-of-function mutations), familial hemiplegic migraine and spinocerebellar ataxia (gain-of-function mutations) (Ophoff et al., 1996; Zhuchenko et al., 1997; Imbrici et al., 2004). $Ca_v2.3^{-/-}$ mice display a predominantly normal phenotype with alterations in glucose metabolism and inflammatory pain responses (Cao, 2006). Injections of peptides into the CNS that block $Ca_v2.1$ and $Ca_v2.3$ channels produce some similar effects (reviewed in Vanegas and Schaible, 2000).

Despite non-selective block of all Ca_v2 subtypes, TROX-1 did not display the deleterious effects associated with $Ca_v2.1$ deletion in mice and mutations in humans. In fact, TROX-1 caused significant analgesic activity at 20-fold lower brain and plasma levels than were required to induce significant impairment of motor coordination in the rota-rod test. We hypothesize that the lack of effect of TROX-1 on motor coordination at concentrations that produce analgesia might result from state-dependent block of Ca_v2 channels in a manner that preferentially affects channel activity in pain signaling pathways. $Ca_v2.1$ currents expressed in cerebellar Purkinje neurons, as well as certain recombinant $Ca_v2.1$ splice variants, are less inactivating than other Ca_v2 family members (Mintz et al., 1992; Bourinet et al., 1999) and may, therefore, have reduced sensitivity for block by state-dependent blockers such as TROX-1.

The clinical validation of $Ca_v2.2$ as a target for the treatment of chronic, severe pain has been

established with the approval of ziconotide. This discovery has sparked great interest in exploiting the full potential of this novel mechanism (reviewed in Miljanich, 2004). Indeed, ziconotide provides pain relief to many people for whom there are no other treatment options. The development of an orally bioavailable, $Ca_v2.2$ blocker with an improved therapeutic window would be another milestone in the treatment options for debilitating pain. There have been a number of previous reports concerning the identification of novel, small organic molecules that block N-type channels and exhibit analgesic and other activities in rodent models (reviewed in Yamamoto and Takahara, 2009). Structurally, there appears to be a wide range of permissive pharmacophores that can functionally interact with the N-type channel complex, including dialkyl-dipeptidylamines, substituted amino acids, imidazolines, saturated and unsaturated hydrocarbons, dihydropyridines, 4-aminopiperidines and di-substituted piperazines (Yamamoto and Takahara, 2009). TROX-1 compares very favorably to these other agents in exhibiting state-dependent Ca_v-2 blockade, being both orally available and brain penetrant, possessing minimal activity against non-Ca_v2 ion channels and other non-specific molecular and physiological targets, and showing broad spectrum analgesic efficacy in wide range of rodent models of chronic pain with efficacy equivalent to pregabalin, duloxetine and naproxen. This is the first study demonstrating that a state-dependent Ca_v2 blocker affords a therapeutic window over cardiovascular and CNS side effects. Overall, the data reported concerning TROX-1 support the notion that an orally administered, state-dependent Ca_v2 blocker may achieve a therapeutic window suitable for the treatment of pain in the clinic.

Acknowledgments

The authors thank L. Gichuru, X. Li, A. M. Ritter, and K. Villa for outstanding technical expertise. The authors also thank K. Rogers and A. Weber for scientific guidance.

References

Bourinet E, Soong TW, Sutton K, Slaymaker S, Mathews E, Monteil A, Zamponi GW, Nargeot J and Snutch TP (1999) Splicing of alpha 1A subunit gene generates phenotypic variants of P- and Q-type calcium channels. *Nat Neurosci* **2**:407-415.

Bowersox SS, Gadbois T, Singh T, Pettus M, Wang YX and Luther RR (1996) Selective N-type neuronal voltage-sensitive calcium channel blocker, SNX-111, produces spinal antinociception in rat models of acute, persistent and neuropathic pain. *J Pharmacol Exp Ther* **279**:1243-1249.

Bowersox SS, Singh T, Nadasdi L, Zukowska-Grojec Z, Valentino K and Hoffman BB (1992) Cardiovascular effects of omega-conopeptides in conscious rats: mechanisms of action. *J Cardiovasc Pharmacol* **20**:756-764.

Cao YQ (2006) Voltage-gated calcium channels and pain. *Pain* **126**:5-9.

Chaplan SR, Bach FW, Pogrel JW, Chung JM and Yaksh TL (1994) Quantitative assessment of tactile allodynia in the rat paw. *J Neurosci Methods* **53**:55-63.

Cizkova D, Marsala J, Lukacova N, Marsala M, Jergova S, Orendacova J and Yaksh TL (2002) Localization of N-type Ca2+ channels in the rat spinal cord following chronic constrictive nerve injury. *Exp Brain Res* **147**:456-463.

Colpaert FC (1987) Evidence that adjuvant arthritis in the rat is associated with chronic pain. *Pain* **28**:201-222.

Dai G, Haedo RJ, Warren VA, Ratliff KS, Bugianesi RM, Rush A, Williams ME, Herrington J, Smith MM, McManus OB and Swensen AM (2008) A high-throughput assay for evaluating state dependence and subtype selectivity of Cav2 calcium channel inhibitors. *Assay Drug Dev Technol* **6**:195-212.

Diaz A and Dickenson AH (1997) Blockade of spinal N- and P-type, but not L-type, calcium channels inhibits the excitability of rat dorsal horn neurones produced by subcutaneous formalin inflammation. *Pain* **69**:93-100.

Doering CJ and Zamponi GW (2003) Molecular pharmacology of high voltage-activated calcium channels. *J Bioenerg Biomembr* **35**:491-505.

Dubel SJ, Starr TV, Hell J, Ahlijanian MK, Enyeart JJ, Catterall WA and Snutch TP (1992) Molecular cloning of the alpha-1 subunit of an omega-conotoxin-sensitive calcium channel. *Proc Natl Acad Sci U S A* **89**:5058-5062.

Evans AR, Nicol GD and Vasko MR (1996) Differential regulation of evoked peptide release by voltage-sensitive calcium channels in rat sensory neurons. *Brain Res* **712**:265-273.

Feigenbaum P, Garcia ML and Kaczorowski GJ (1988) Evidence for distinct sites coupled to high affinity omega-conotoxin receptors in rat brain synaptic plasma membrane vesicles. *Biochem Biophys Res Commun* **154**:298-305.

Heinke B, Balzer E and Sandkuhler J (2004) Pre- and postsynaptic contributions of voltage-dependent Ca2+ channels to nociceptive transmission in rat spinal lamina I neurons. *Eur J Neurosci* **19**:103-111.

Imbrici P, Jaffe SL, Eunson LH, Davies NP, Herd C, Robertson R, Kullmann DM and Hanna MG (2004) Dysfunction of the brain calcium channel Cav2.1 in absence epilepsy and episodic ataxia. *Brain* **127**:2682-2692.

Ino M, Yoshinaga T, Wakamori M, Miyamoto N, Takahashi E, Sonoda J, Kagaya T, Oki T, Nagasu T, Nishizawa Y, Tanaka I, Imoto K, Aizawa S, Koch S, Schwartz A, Niidome T, Sawada K and Mori Y (2001) Functional disorders of the sympathetic nervous system in mice lacking the alpha 1B subunit (Cav 2.2) of N-type calcium channels. *Proc Natl Acad Sci U S A* **98**:5323-5328.

Jun K, Piedras-Renteria ES, Smith SM, Wheeler DB, Lee SB, Lee TG, Chin H, Adams ME, Scheller RH, Tsien RW and Shin HS (1999) Ablation of P/Q-type Ca(2+) channel currents, altered synaptic transmission, and progressive ataxia in mice lacking the alpha(1A)-subunit. *Proc Natl Acad Sci U S A* **96**:15245-15250.

Kim C, Jun K, Lee T, Kim SS, McEnery MW, Chin H, Kim HL, Park JM, Kim DK, Jung SJ, Kim J and Shin HS (2001) Altered nociceptive response in mice deficient in the alpha(1B) subunit of the voltage-dependent calcium channel. *Mol Cell Neurosci* **18**:235-245.

Kim SH and Chung JM (1992) An experimental model for peripheral neuropathy produced by segmental spinal nerve ligation in the rat. *Pain* **50**:355-363.

Kuwayama H and Kanazawa T (1982) Purification of cardiac sarcolemmal vesicles: high sodium pump content and ATP-dependent, calmodulin-activated calcium uptake. *J Biochem* **91**:1419-1426.

Leppard P, Faris I, Jamieson GG and Ludbrook J (1979) A method for the analysis of sigmoid stimulus-response curves. *Aust J Exp Biol Med Sci* **57**:39-41.

Malmberg AB and Yaksh TL (1995) Effect of continuous intrathecal infusion of omega-conopeptides, N-type calcium-channel blockers, on behavior and antinociception in the formalin and hot-plate tests in rats. *Pain* **60**:83-90.

Miljanich GP (2004) Ziconotide: neuronal calcium channel blocker for treating severe chronic pain. *Curr Med Chem* **11**:3029-3040.

Mintz IM, Adams ME and Bean BP (1992) P-type calcium channels in rat central and peripheral neurons. *Neuron* **9**:85-95.

Mori Y, Nishida M, Shimizu S, Ishii M, Yoshinaga T, Ino M, Sawada K and Niidome T (2002) Ca2+ channel alpha(1B) subunit (Cav 2.2) knockout mouse reveals a predominant role of N-type channels in the sympathetic regulation of the circulatory system. *Trends Cardiovasc Med* **12**:270-275.

Motin L and Adams DJ (2008) omega-Conotoxin inhibition of excitatory synaptic transmission evoked by dorsal root stimulation in rat superficial dorsal horn. *Neuropharmacology* **55**:860-864.

Olivera BM, Miljanich GP, Ramachandran J and Adams ME (1994) Calcium channel diversity and neurotransmitter release: the omega-conotoxins and omega-agatoxins. *Annu Rev Biochem* **63**:823-867.

Ophoff RA, Terwindt GM, Vergouwe MN, van Eijk R, Oefner PJ, Hoffman SM, Lamerdin JE, Mohrenweiser HW, Bulman DE, Ferrari M, Haan J, Lindhout D, van Ommen GJ, Hofker MH, Ferrari MD and Frants RR (1996) Familial hemiplegic migraine and episodic ataxia type-2 are caused by mutations in the Ca2+ channel gene CACNL1A4. *Cell* **87**:543-552.

Pruneau D and Belichard P (1992) Haemodynamic and humoral effects of omega-conotoxin GVIA in normotensive and spontaneously hypertensive rats. *Eur J Pharmacol* **211**:329-335.

Scott DA, Wright CE and Angus JA (2002) Actions of intrathecal omega-conotoxins CVID, GVIA, MVIIA, and morphine in acute and neuropathic pain in the rat. *Eur J Pharmacol* **451**:279-286.

Tsukamoto M, Kiso T, Shimoshige Y, Aoki T, Nobuya M (2010) Spinal mechanism of standard analgesics: Evaluation using mouse models of allodynia. *Eur. J. Pharmacol.* **634**: 40-45.

Vanegas H and Schaible H (2000) Effects of antagonists to high-threshold calcium channels upon spinal mechanisms of pain, hyperalgesia and allodynia. *Pain* **85**:9-18.

Vyklicky L, Rudomin P, Zajac FE, 3rd and Burke RE (1969) Primary afferent depolarization evoked by a painful stimulus. *Science* **165**:184-186.

Wang YX, Gao D, Pettus M, Phillips C and Bowersox SS (2000) Interactions of intrathecally administered ziconotide, a selective blocker of neuronal N-type voltage-sensitive calcium channels, with morphine on nociception in rats. *Pain* **84**:271-281.

Westenbroek RE, Hoskins L and Catterall WA (1998) Localization of Ca2+ channel subtypes on rat spinal motor neurons, interneurons, and nerve terminals. *J Neurosci* **18**:6319-6330.

Williams ME, Brust PF, Feldman DH, Patthi S, Simerson S, Maroufi A, McCue AF, Velicelebi G, Ellis SB and Harpold MM (1992) Structure and functional expression of an omega-conotoxin-sensitive human N-type calcium channel. *Science* **257**:389-395.

Winquist RJ, Pan JQ, and Gribkoff VK (2005) Use-dependent blockade of Cav2.2 voltage-gated calcium channels for neuropathic pain. *Biochem Pharmacol* **70**:489-499.

Wright CE, Hawkes AL and Angus JA (2000) Postural hypotension following N-type Ca2+ channel blockade is amplified in experimental hypertension. *J Hypertens* **18**:65-73.

Yamamoto T and Takahara A (2009) Recent updates of N-type calcium channel blockers with therapeutic potential for neuropathic pain and stroke. *Curr Top Med Chem* **9**:377-395.

Zhuchenko O, Bailey J, Bonnen P, Ashizawa T, Stockton DW, Amos C, Dobyns WB, Subramony SH, Zoghbi HY and Lee CC (1997) Autosomal dominant cerebellar ataxia (SCA6) associated with small polyglutamine expansions in the alpha 1A-voltage-dependent calcium channel. *Nat Genet* **15**:62-69.

Footnotes

Address correspondence to: Dr. Joseph L. Duffy, Merck Research Laboratories, PO Box 2000, Rahway, NJ 07065. E-mail: joseph_duffy@merck.com

JPET Fast Forward. Published on May 3, 2010 as DOI: 10.1124/jpet.110.166363
This article has not been copyedited and formatted. The final version may differ from this version.

Legends for Figures

Fig. 1. State-dependent block of $Ca_v2.2$ channels by TROX-1. TROX-1 preferentially blocked recombinant $Ca_v2.2$ channels under depolarized conditions (A) compared with hyperpolarized conditions (B) in a fluorescent calcium influx assay. Block of $Ca_v2.2$ channels in rat dorsal root ganglion neurons in electrophysiological experiments is shown in (C). TROX-1 preferentially blocks channels at depolarized membrane potentials (-50 to -70 mV; circles) compared with hyperpolarized potentials (-100 mV; squares). Representative currents displaying block by 3 μM TROX-1 at depolarized and hyperpolarized potentials are shown at right for two cells.

Fig. 2. TROX-1 block of Ca_v2 family channels in rat dorsal root ganglion (DRG) neurons measured with calcium imaging. Calcium influx was initiated by elevation of bath potassium concentration from 14 mM to 72 mM for two minutes (triangles). Peak calcium signals were blocked by a combination of GVIA, ω-Agatoxin IVA and SNX-482 (81%: A). TROX-1 reversibly and fully inhibited the peak calcium signals in a single DRG neuron (B). A dose-response curve was constructed from average responses in 8 neurons from 4 experiments and plotted in (C). Solid line represents a fit to the data using a Hill equation with an IC50 value of 2.1 μM, a Hill slope of 1.1 and a maximum inhibition of 0.99.

Fig. 3. ^{125}I-CgTX GVIA binding site density in rat lumbar spinal cord segments. Comparison of complete Freund's adjuvant (CFA)-induced ^{25}I-CgTX GVIA binding in rat lumbar membrane vesicles ipsilateral to CFA treatment as compared with the contralateral side. Connected symbols are from individual experiments.

Fig. 4. Analgesic activity of TROX-1 in rodent pain models. In the rat complete Freund's adjuvant (CFA)-induced hyperalgesia model (A and B), TROX-1 dose-dependently reversed CFA-induced hyperalgesia with a duration of action greater than 8 hr post-dose (A). Anti-hyperalgesic effects of TROX-1 and standard analgesics at 1 hr post-dose in the rat CFA model, expressed as % reversal of hyperalgesia calculated as indicated in Methods (B). TROX-1 inhibited rat capsaicin-induced secondary allodynia similar to pregabalin and duloxetine at 1 hr post-dose (C). TROX-1 dose-

dependently reversed rat Spinal Nerve Ligation (SNL)-induced allodynia with a duration of action greater than 8 hr post-dose (D), and its anti-allodynic properties were comparable to pregabalin or duloxetine at 1 hr post-dose (E). The compounds used for neuropathic pain in SNL model vs. rota-rod model of motor-coordination were compared with TROX-1 (E). Pregabalin and duloxetine induced significant impairment of motor-coordination (>20%) at lower doses than TROX-1, as represented by the region in red. Mice deficient for $Ca_v2.2$ showed greater thermal threshold both in the absence of inflammation (pre-CFA) and 1 day following intra-dermal CFA administration as compared to wild-type mice (F). At 1 hr post-dose, TROX-1 significantly reversed CFA-induced hyperalgesia in wild-type mice (88% reversal, F), but not in $Ca_v2.2$ deficient mice (31% reversal, F). Significance ($n \geq 6$/group) was calculated using a 2-way ANOVA followed by a Bonferroni post-hoc tests for multiple comparisons to "vehicle" values (*$p<0.05$).

Fig. 5. Effects of a 3 day chronic treatment of TROX-1 and naproxen in the complete Freund's adjuvant (CFA)-induced hyperalgesia model in rats. Percent Reversal of hypersensitivity (indicated above bars) was calculated as indicated in Methods.

Fig. 6. Anti-hyperalgesic effects of TROX-1 in the rat knee iodoacetate (IOA) model of inflammatory pain. TROX-1 reversed IOA-induced allodynia (A) and weight-bearing behavior (B) in a dose-dependent manner.

Fig. 7. Effects of TROX-1 and morphine in the rat hot plate model of acute nociception. Morphine (10 mg/kg) significantly enhanced latency while TROX-1 (10 mg/kg and 30 mg/kg) was inactive.

Fig. 8. Comparison of the analgesic activity of TROX-1 vs. side effect profile. TROX-1 ED_{50} value in rat models of inflammatory or neuropathic pain was 1 μM. Significant impairment (>20%) of motor-coordination in the rat rota-rod assay corresponded to plasma levels of 20 μM (A). Significant canine cardiovascular changes were observed at plasma levels of 40 μM (B).

JPET Fast Forward. Published on May 3, 2010 as DOI: 10.1124/jpet.110.166363
This article has not been copyedited and formatted. The final version may differ from this version.

Fig. 9. Representative baroreflex curves showing the effects of GVIA and TROX-1 on rat baroreflex function. GVIA IV (3 μg/kg IV) decreased heart rate range and baroreflex sensitivity in an individual animal (A). TROX-1 (1 mg/kg IV) showed a modest effect on heart rate range only (B). Measurements were made before treatment (Control, filled circles) and 30 min after treatment with GVIA (A, open circles) or TROX-1 (B, open circles).

JPET Fast Forward. Published on May 3, 2010 as DOI: 10.1124/jpet.110.166363
This article has not been copyedited and formatted. The final version may differ from this version.

Tables

Table 1. Effect of Cav2 channel toxins on neonatal rat DRG calcium influx

Treatment	Percent Inhibition	n
ω-Conotoxin GVIA	34 ± 4	44
ω-Agatoxin IVA	20 ± 3	52
SNX-482	9 ± 3	26
ω-Conotoxin GVIA + ω -Agatoxin IVA	65 ± 7	11
ω-Conotoxin GVIA + SNX-482	54 ± 5	10
ω-Agatoxin IVA + SNX-482	42 ± 6	38
ω-Conotoxin GVIA + ω-Agatoxin IVA + SNX-482	75 ± 1	43

JPET Fast Forward. Published on May 3, 2010 as DOI: 10.1124/jpet.110.166363
This article has not been copyedited and formatted. The final version may differ from this version.

Table 2. TROX-1 selectivity over ancillary ion channel targets

Ion Channel	IC_{50} (μM)	Assay type
$Ca_v1.2$	18	Fluorescent/calcium influx
$Ca_v3.1$	15	Fluorescent/calcium influx
$Ca_v3.2$	>20	Fluorescent/calcium influx
$Na_v1.7$	3.3	Fluorescent/membrane potential
$Na_v1.8$	2.6	Fluorescent/membrane potential
$Na_v1.5$	29	Voltage clamp
I_{kr}	6	Voltage clamp
I_{ks}	>30	Voltage clamp

Table 3. Changes in baro-reflex parameters following infusion of TROX-1 in conscious rats

		Vehicle	GVIA (mg/kg)		TROX-1 (mg/kg/min x 30 min)		
			1	3	0.1	0.3	1
Gain	pre-treatment (beats/min/mm Hg)	-2.6 ± 0.19	-2.7 ± 0.34	-2.6 ± 0.41	-3.0 ± 0.44	-4.9 ± 0.26	-4.9 ± 1.10
	post-treatment (% of pre-treatment)	119 ± 11	113 ± 25	73 ± 9 *	144 ± 27	103 ± 23	101 ± 5
BP_{50}	pre-treatment (mm Hg)	126 ± 12	116 ± 2	124 ± 3	115 ± 7	115 ± 4	118 ± 2
	post-treatment (% of pre-treatment)	93 ± 4	101 ± 5	92 ± 4	102 ± 6	99 ± 4	90 ± 5
HR range	pre-treatment (beats/min)	174 ± 47	200 ± 12	177 ± 16	207 ± 21	192 ± 11	209 ± 12
	post-treatment (% of pre-treatment)	86 ± 2	88 ± 8	50 ± 8 *	123 ± 13	130 ± 3	79 ± 5 *
HR min	pre-treatment (beats/min)	312 ± 10	317 ± 17	362 ± 13	289 ± 20	343 ± 12	325 ± 7
	post-treatment (% of pre-treatment)	116 ± 2	109 ± 6	104 ± 2	92 ± 9	89 ± 2	102 ± 1
Plasma Levels (μM)		-	-	-	2.5 ± 0.5	14 ± 2.5	38 ± 4.5

JPET Fast Forward. Published on May 3, 2010 as DOI: 10.1124/jpet.110.166363
This article has not been copyedited and formatted. The final version may differ from this version.

Table 4. Changes in cardiovascular parameters following infusion of TROX-1 in anesthetized dogs

	Baseline	% of Baseline		
		Cumulative dose (mg/kg IV)		
	0	1	3	10
Mean arterial pressure	135 ± 8 mm Hg	96 ± 8	90 ± 7	75 ± 5
Heart rate	151 ± 11 beats/min	90 ± 3	84 ± 4	80 ± 4
PR	91 ± 10 ms	107 ± 2	109 ± 3	107 ± 5
QRS	49 ± 1 ms	100 ± 2	102 ± 3	103 ± 2
QTc	390 ± 2 ms	101 ± 1	101 ± 1	101 ± 2
Plasma levels (μM)		11 ± 4	18 ± 7	55 ± 21

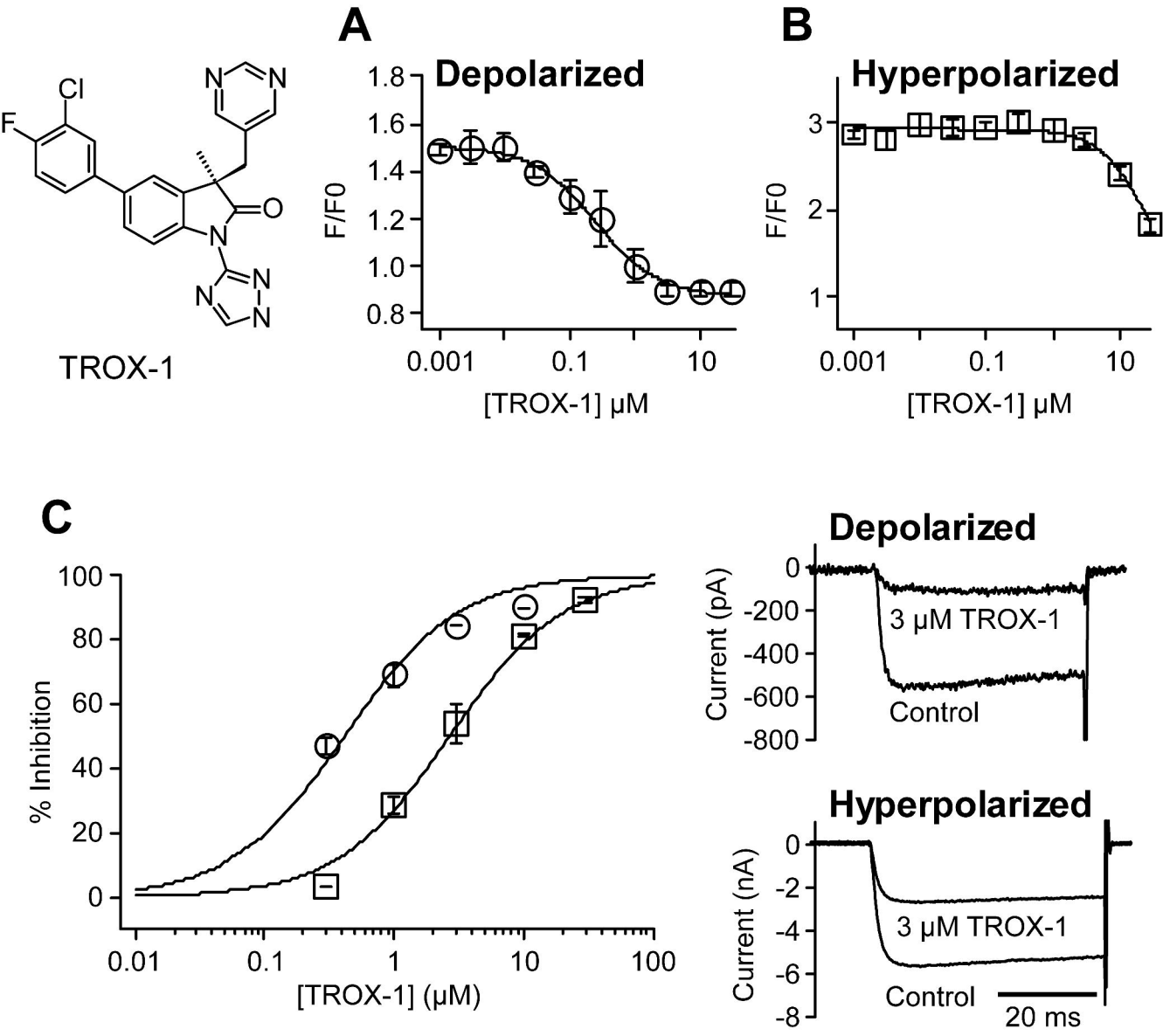

JPET/2010/166363 Figure 1

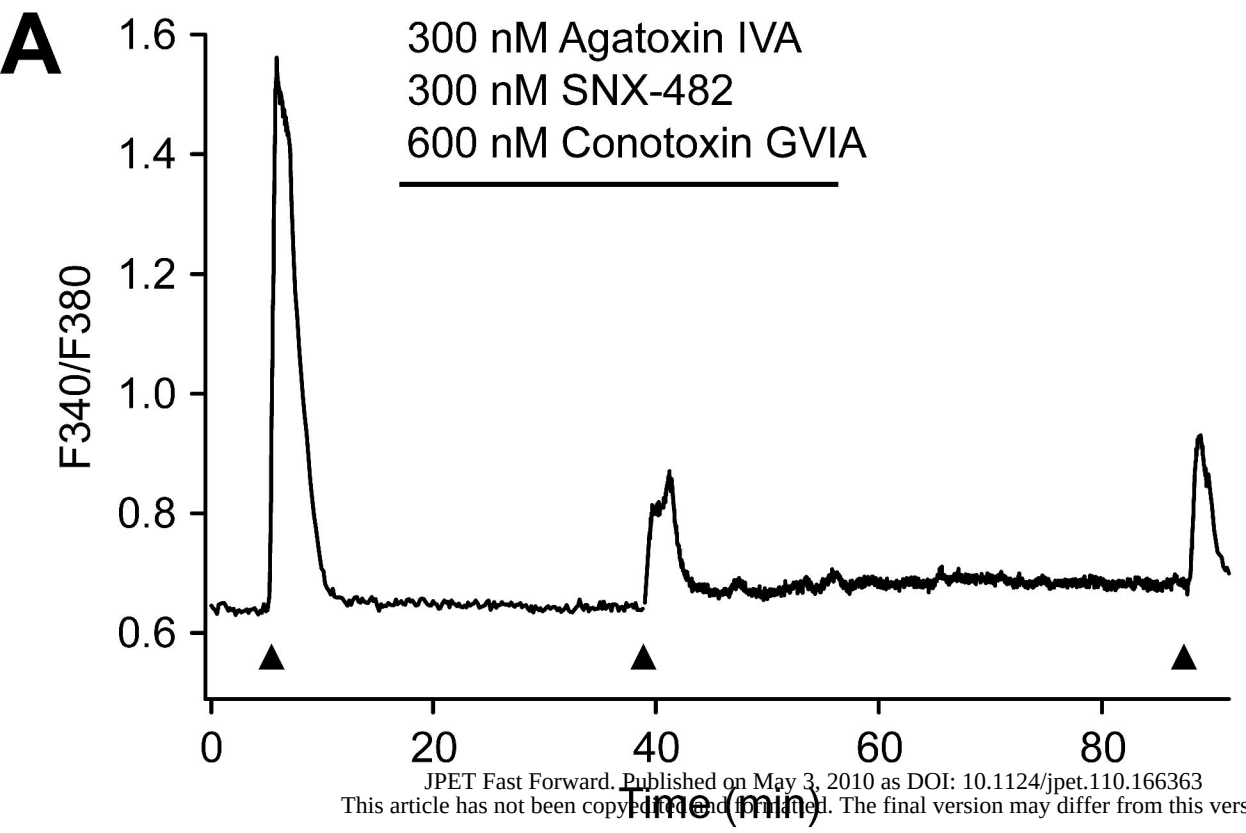

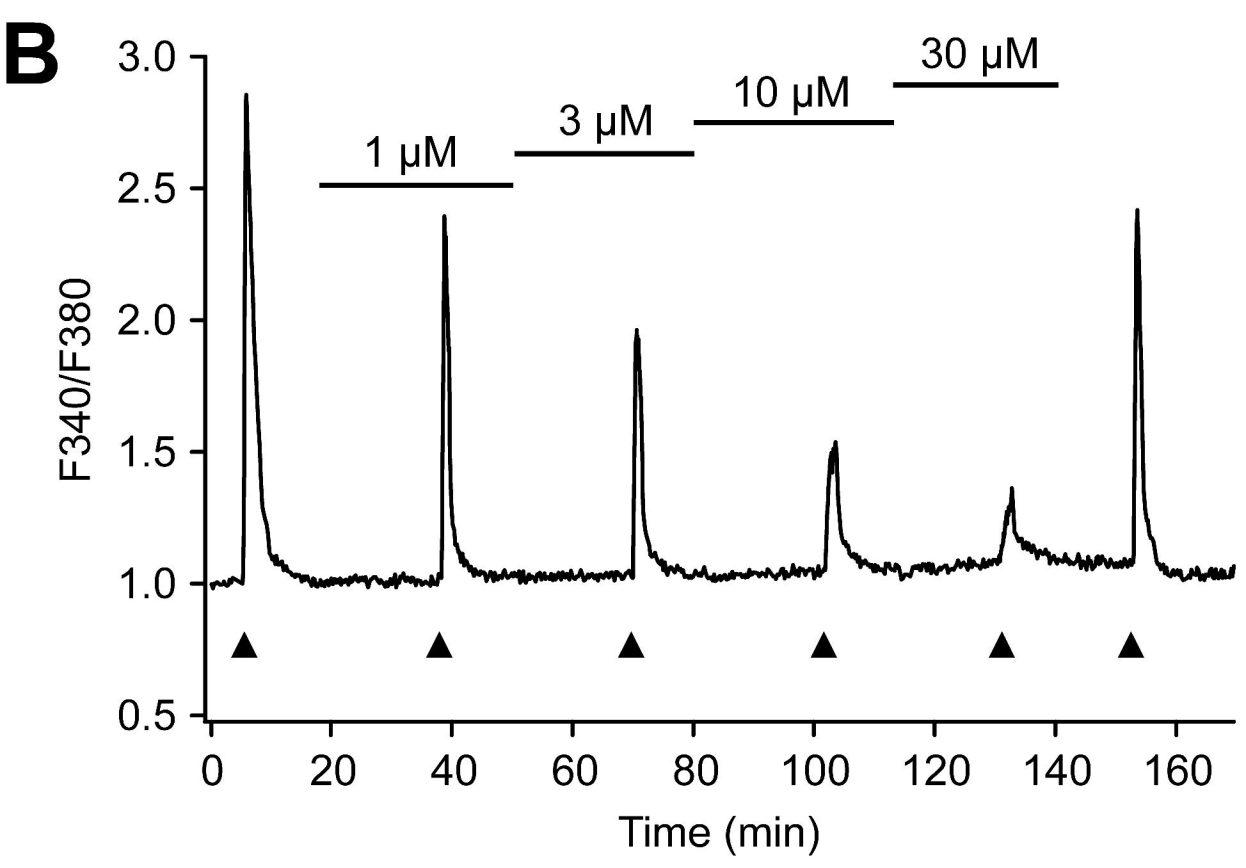

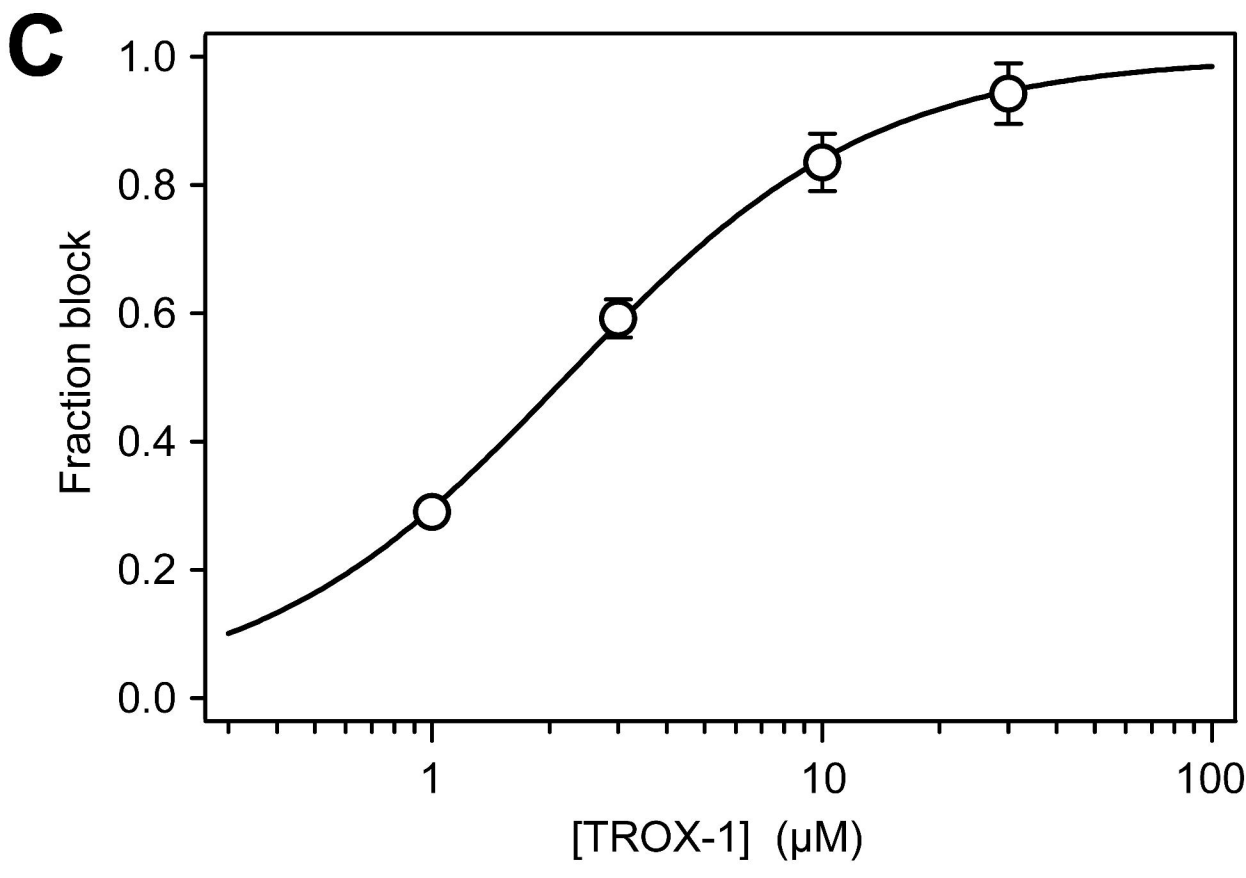

JPET/2010/166363 Figure 2

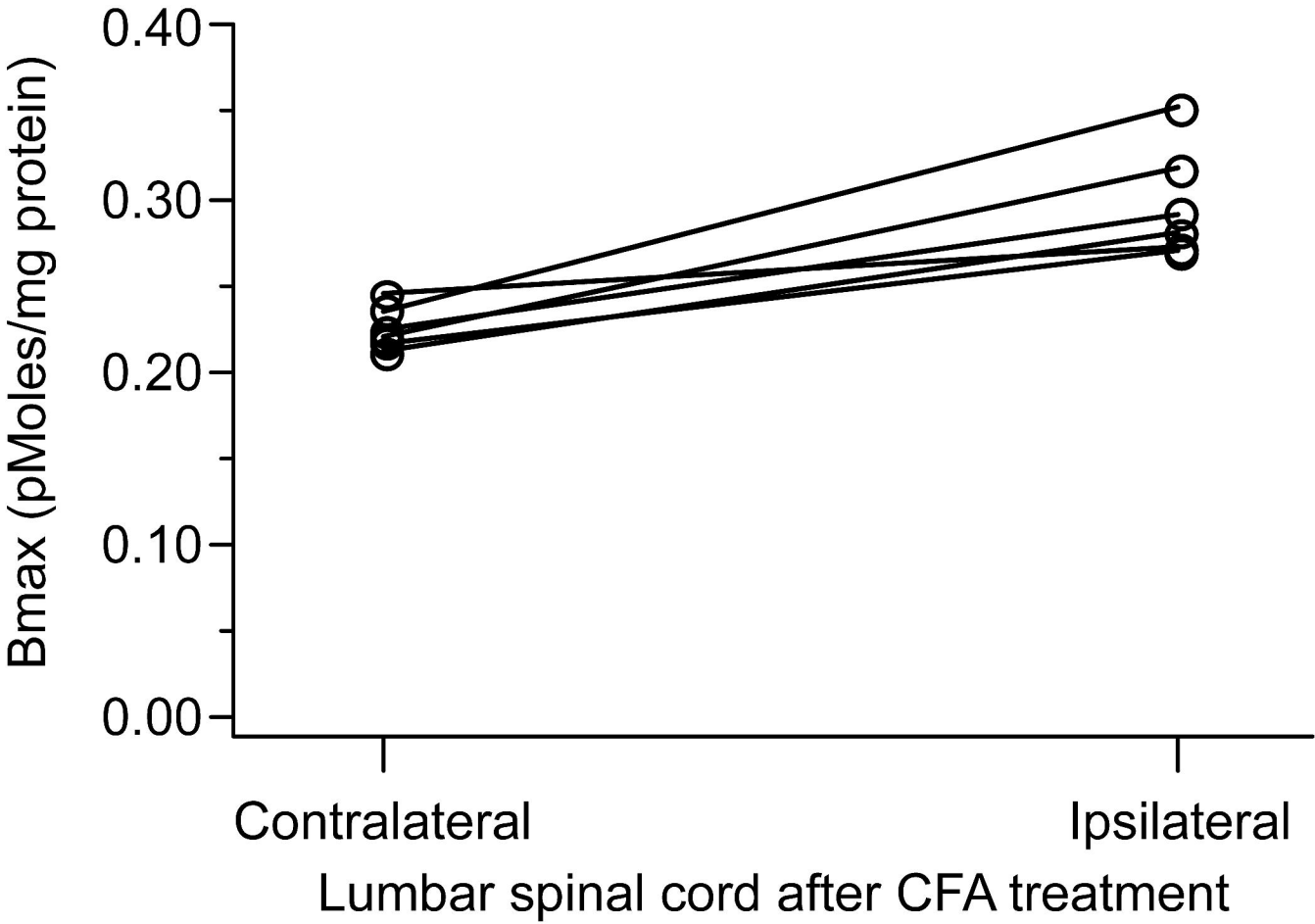

JPET/2010/166363 Figure 3

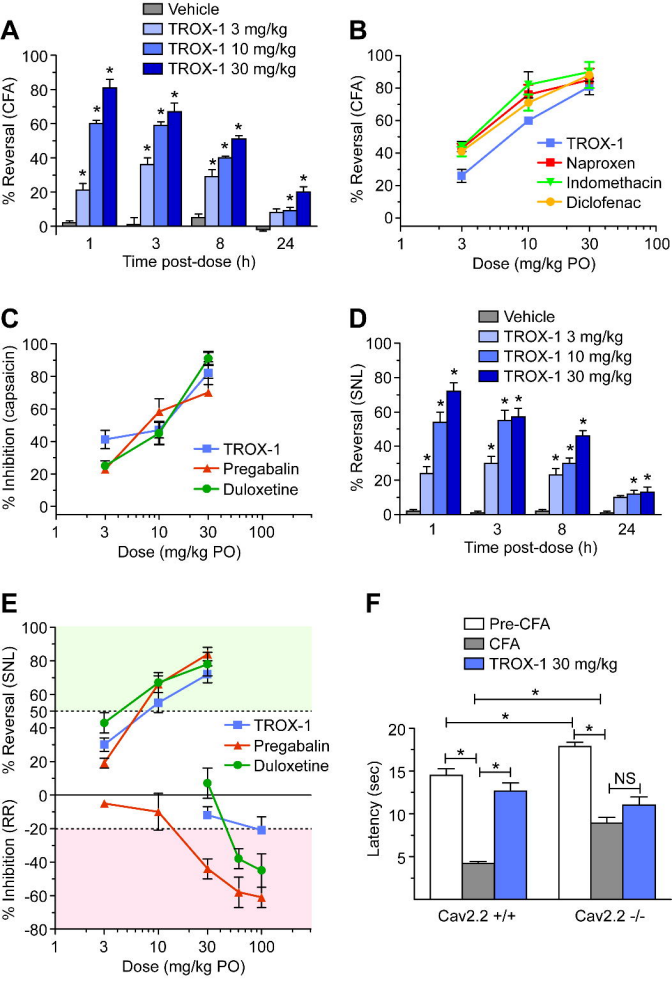

JPET/2010/166363 Figure 4

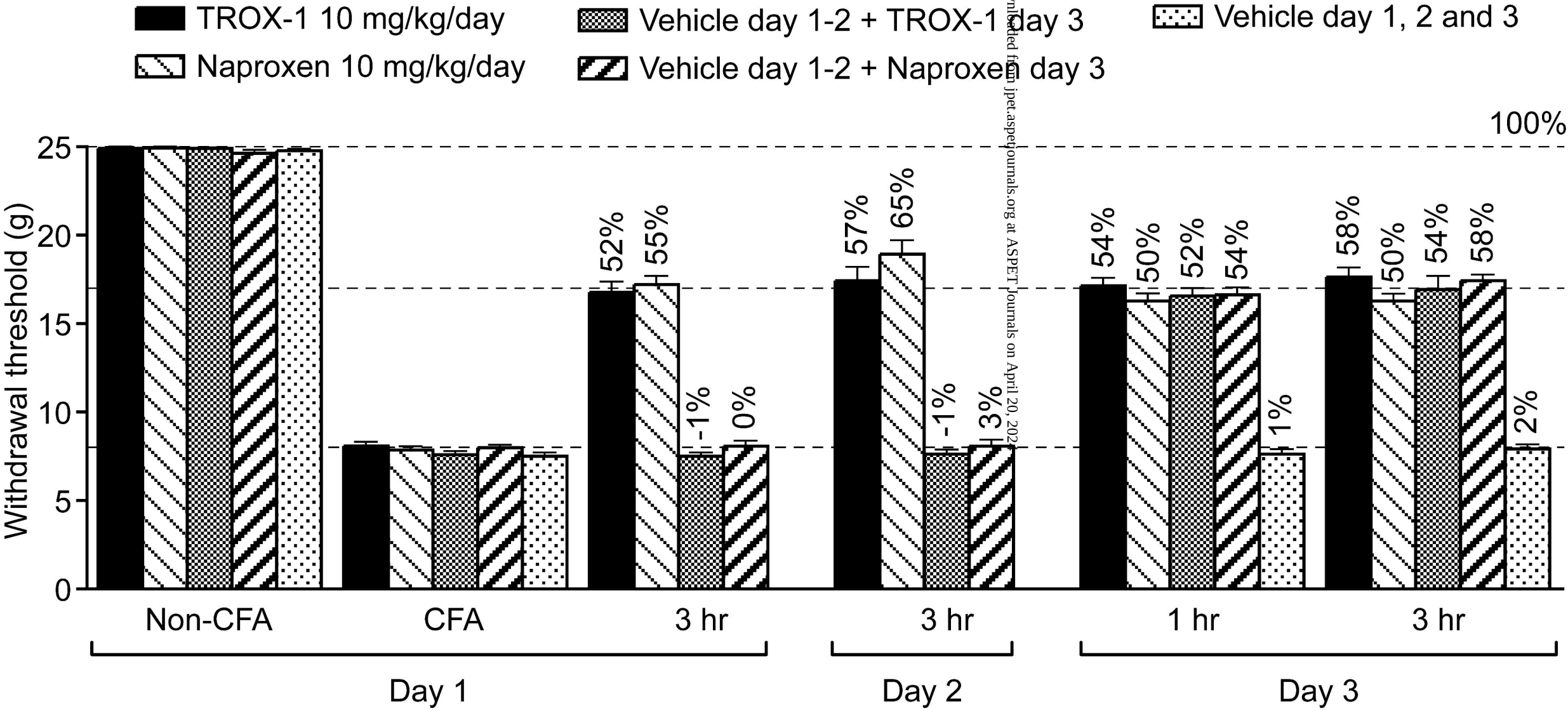

JPET/2010/166363 Figure 5

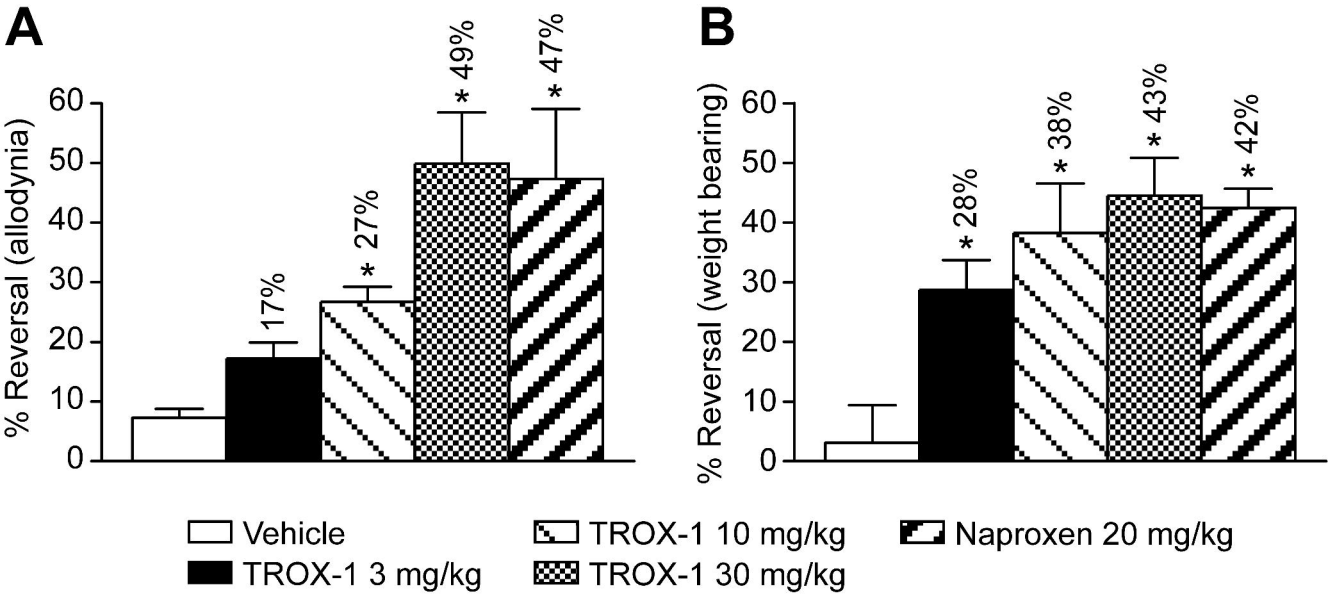

JPET/2010/166363 Figure 6

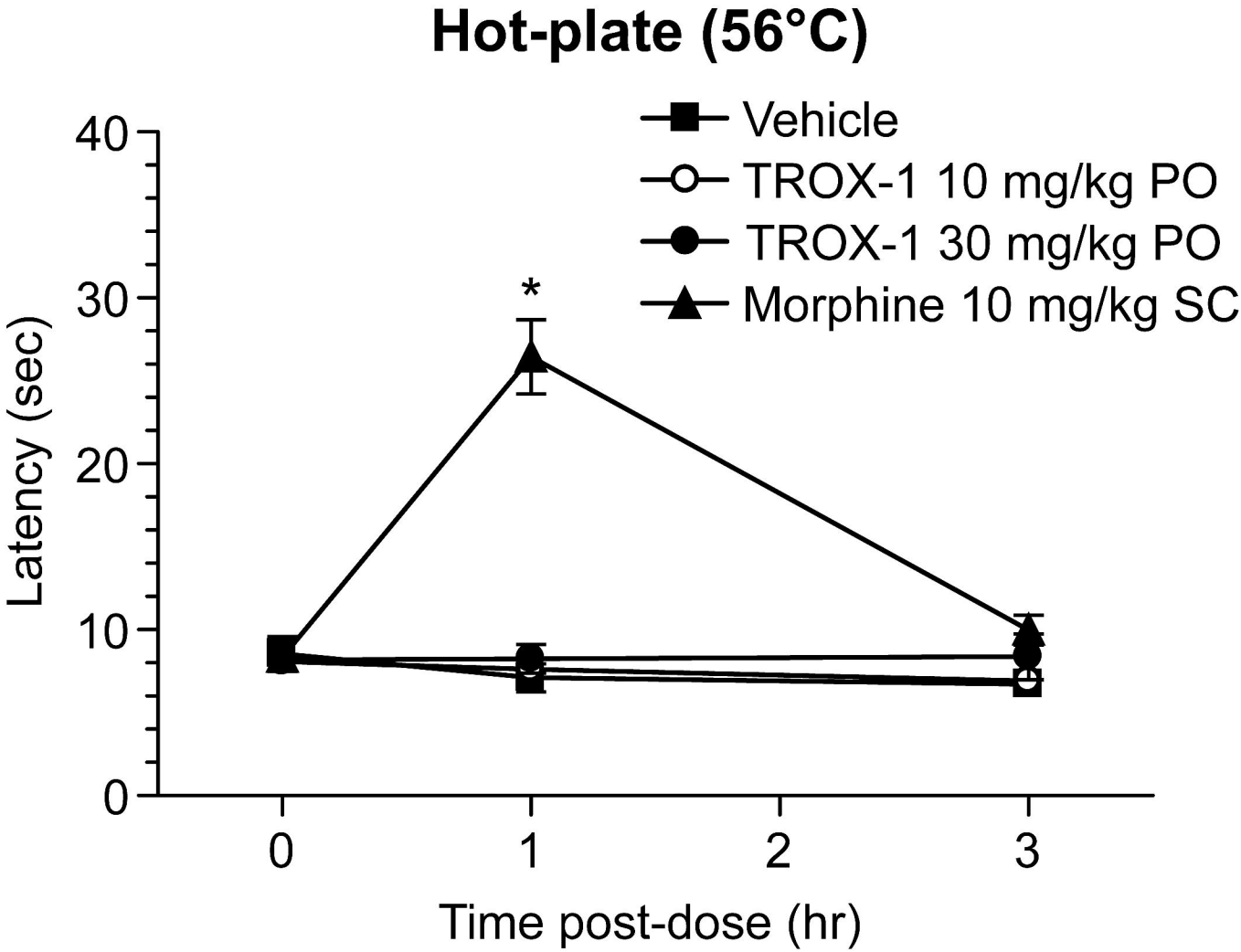

JPET/2010/166363 Figure 7

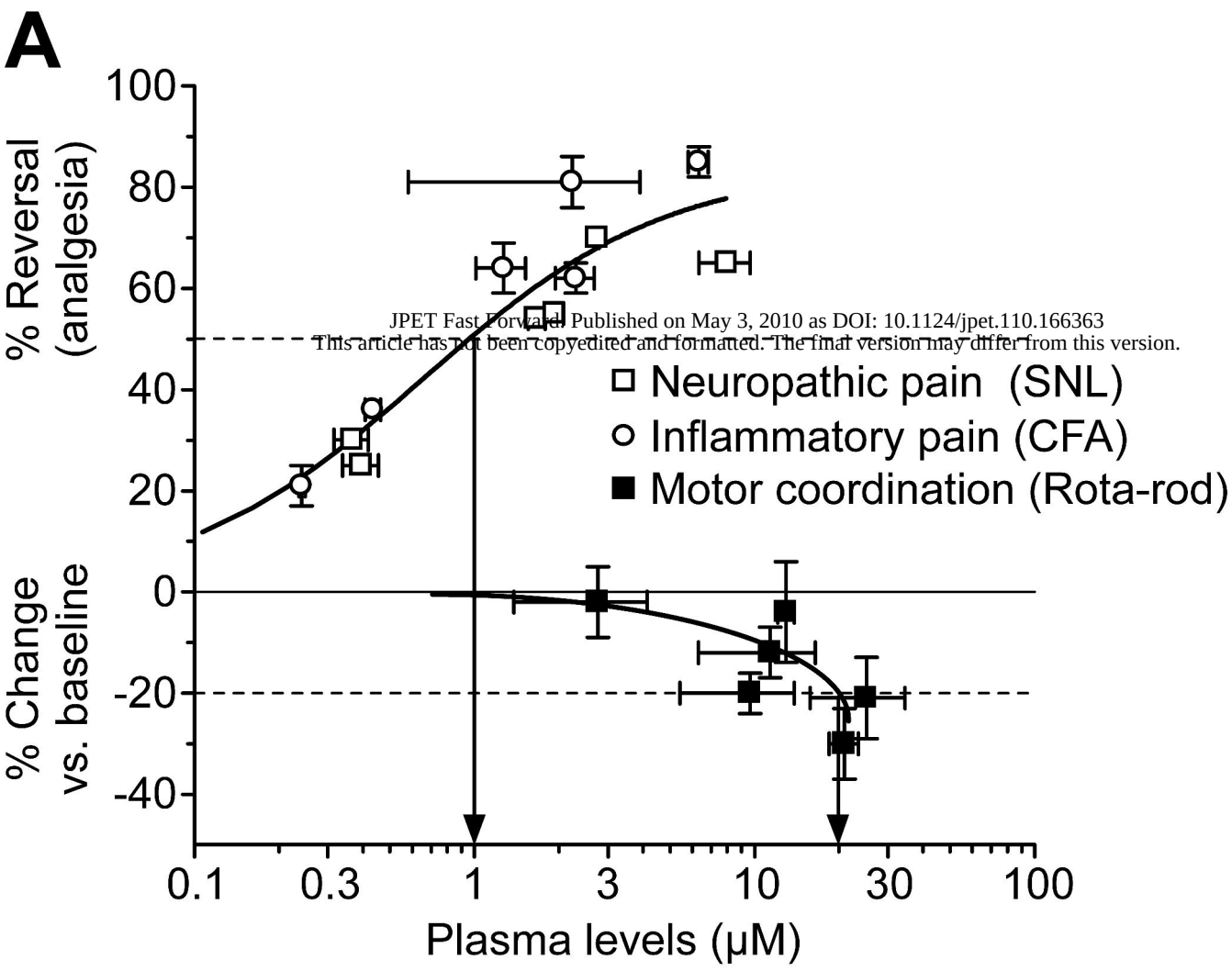

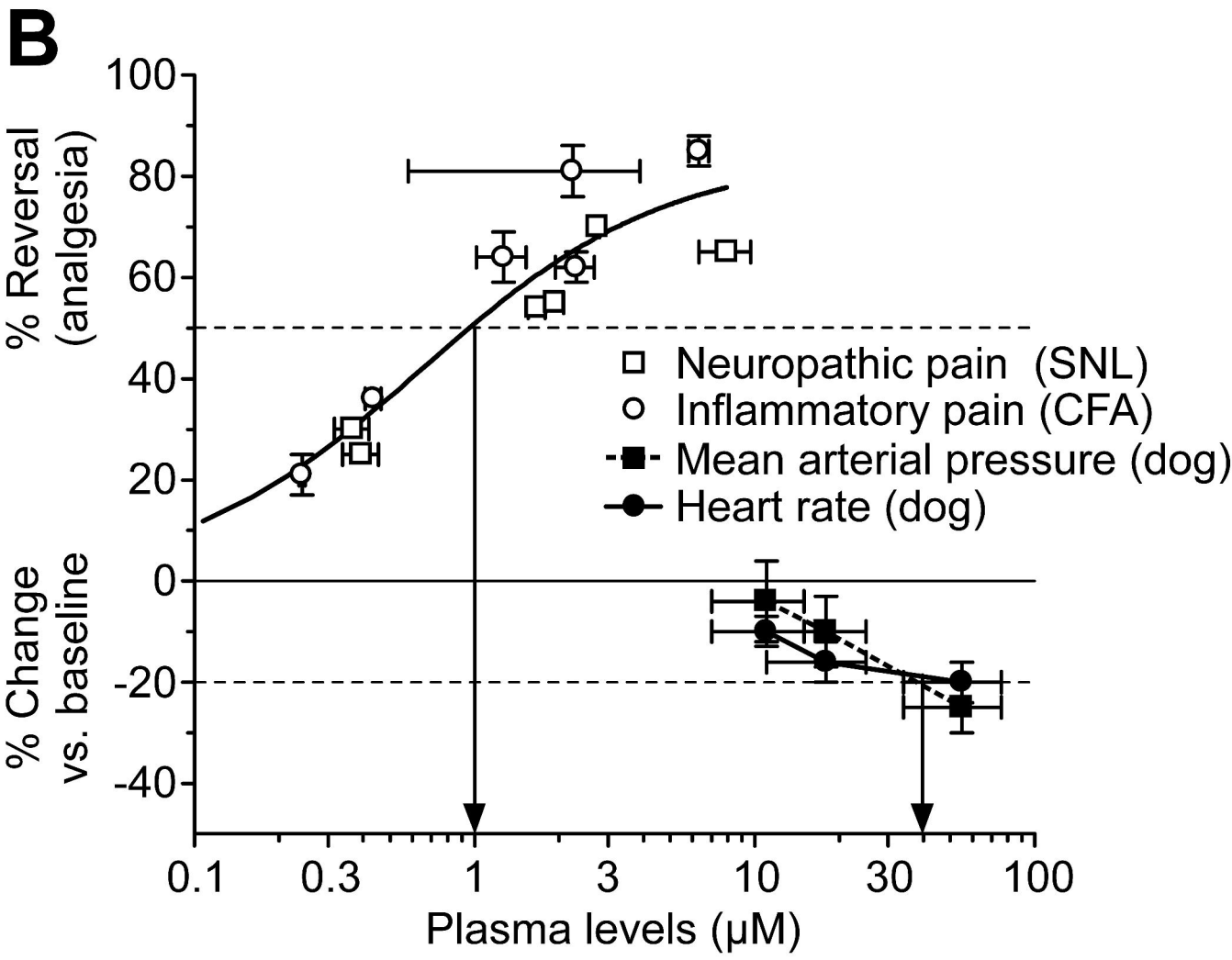

JPET/2010/166363 Figure 8

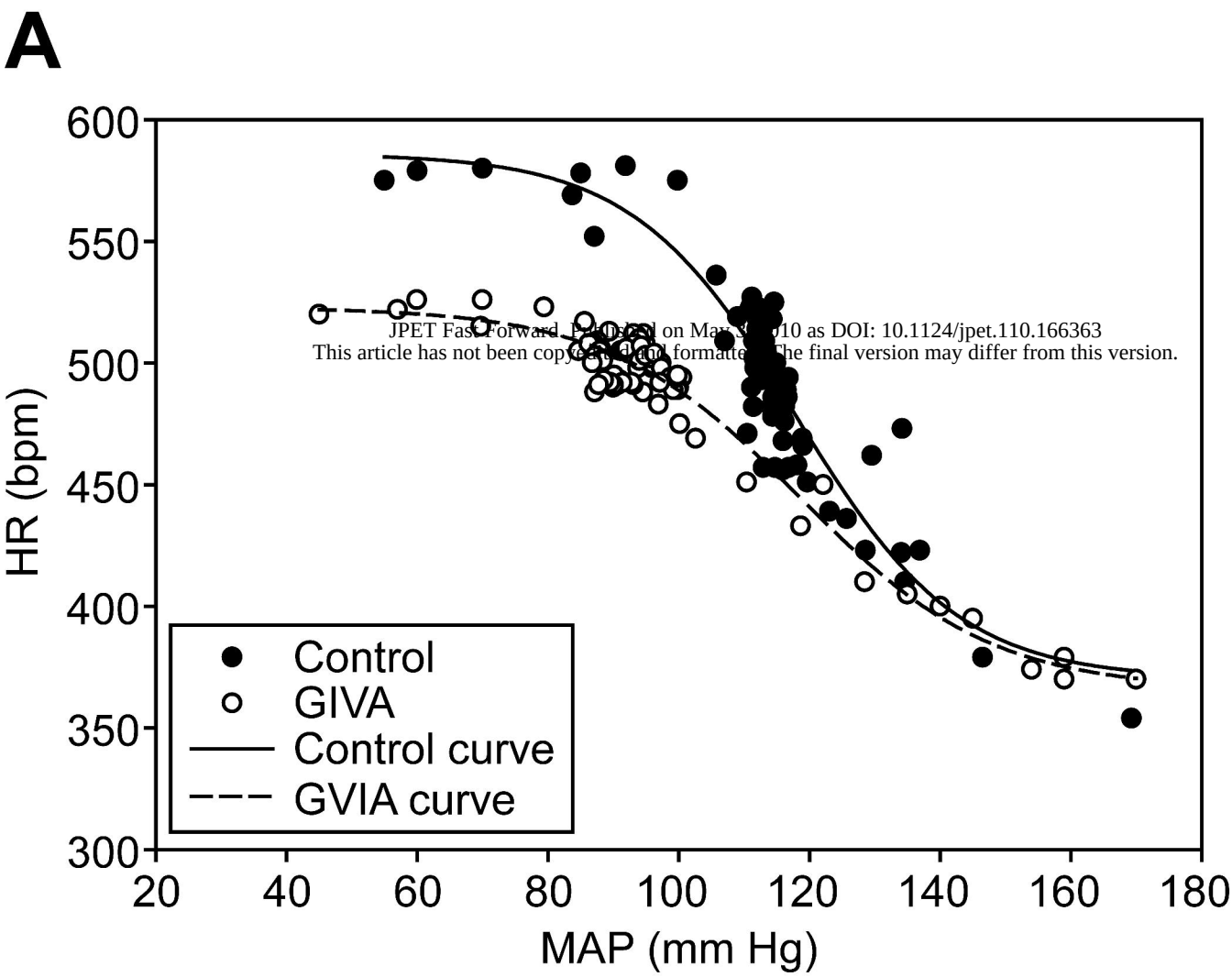

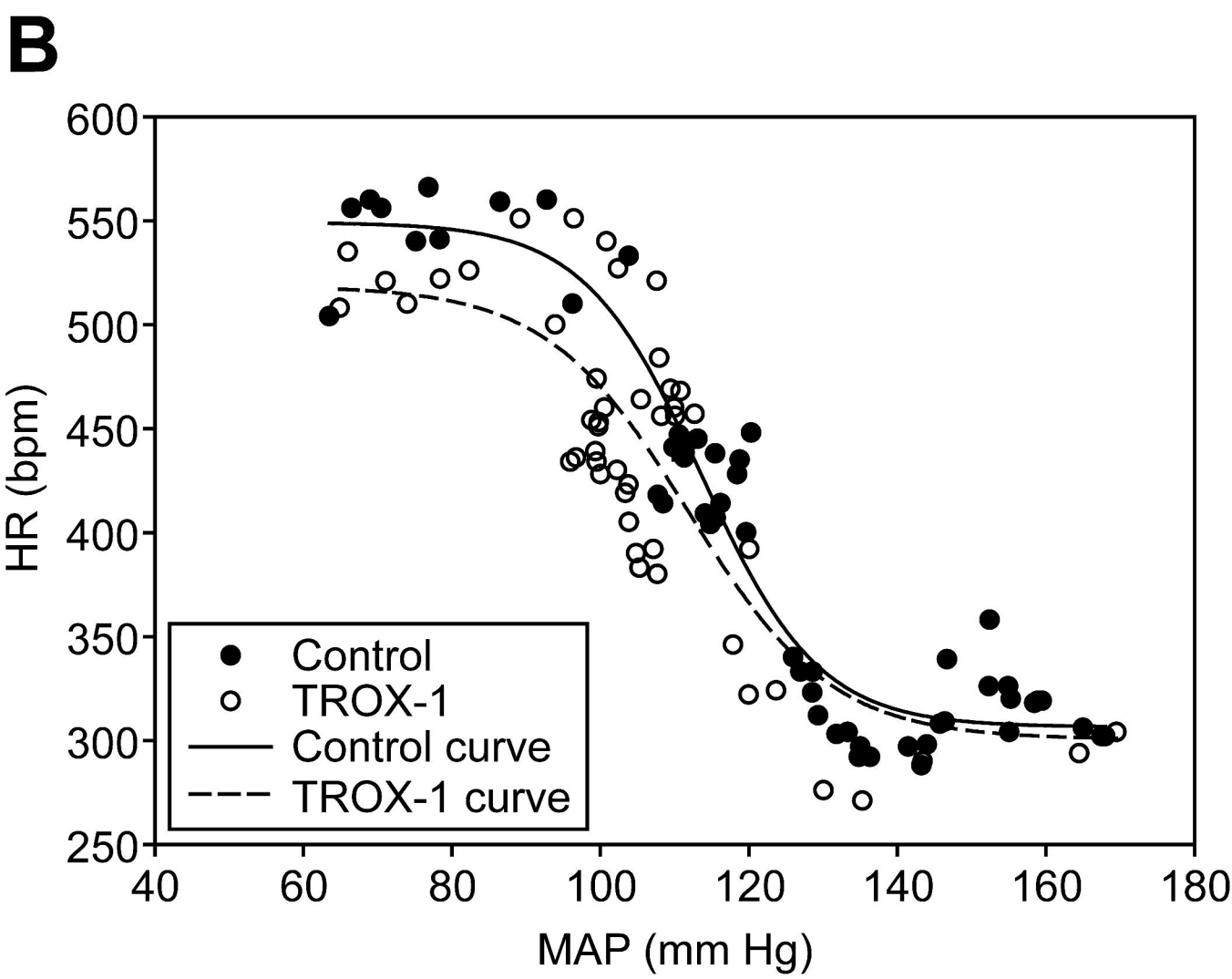

JPET/2010/166363 Figure 9